British Journal of Pharmacology

British Journal of Pharmacology (2016) **173** 2369–2389 2369

RESEARCH PAPER

Capsaicin induces browning of white adipose tissue and counters obesity by activating TRPV1 channel-dependent mechanisms

Correspondence Assistant Professor Baskaran Thyagarajan, University of Wyoming School of Pharmacy, 1000 East University Avenue, Laramie, WY 82071, USA. E-mail: bthyagar@uwyo.edu

Received 5 January 2016; **Revised** 27 April 2016; **Accepted** 30 April 2016

Padmamalini Baskaran, Vivek Krishnan, Jun Ren and Baskaran Thyagarajan

School of Pharmacy, University of Wyoming, Laramie, WY, USA

BACKGROUND AND PURPOSE

The growing epidemic of obesity and metabolic diseases necessitates the development of novel strategies to prevent and treat such diseases. Current research suggests that browning of white adipose tissue (WAT) promotes energy expenditure to counter obesity. Recent research suggests that activation of the TRPV1 channels counters obesity. However, the mechanism by which activation of TRPV1 channels counters obesity still remains unclear.

EXPERIMENTAL APPROACH

We evaluated the effect of dietary capsaicin to induce a browning program in WAT by activating TRPV1 channels to prevent diet-induced obesity using wild-type and TRPV1$^{-/-}$ mouse models. We performed experiments using preadipocytes and fat pads from these mice.

KEY RESULTS

Capsaicin stimulated the expression of brown fat-specific thermogenic uncoupling protein-1 and bone morphogenetic protein-8b in WAT. Capsaicin triggered browning of WAT by promoting sirtuin-1 expression and activity via TRPV1 channel-dependent elevation of intracellular Ca^{2+} and phosphorylation of Ca^{2+}/calmodulin-activated protein kinase II and AMP-activated kinase. Capsaicin increased the expression of PPARγ 1 coactivator α and enhanced metabolic and ambulatory activity. Further, capsaicin stimulated sirtuin-1-dependent deacetylation of PPARγ and the transcription factor PRDM-16 and facilitated PPARγ–PRDM-16 interaction to induce browning of WAT. Dietary capsaicin did not protect TRPV1$^{-/-}$ mice from obesity.

CONCLUSIONS AND INTERPRETATIONS

Our results show for the first time that activation of TRPV1 channels by dietary capsaicin triggers browning of WAT to counteract obesity. Our results suggest that activation of TRPV1 channels is a promising strategy to counter obesity.

Abbreviations

AMPK, AMP-activated kinase; BMP8b, bone morphogenetic protein 8b; brite, brown in white; CAP, capsaicin; CaMKII, Ca^{2+}/calmodulin-activated protein kinase; EF, epididymal fat; FSK, forskolin; HFD, high-fat diet; NCD, normal chow diet; PGC-1α, PPARγ 1 coactivator α; PRDM-16, positive regulatory domain containing 16; SCF, subcutaneous (inguinal) fat; SIRT-1, sirtuin 1; UCP-1, uncoupling protein 1; WAT, white adipose tissue

DOI:10.1111/bph.13514

Tables of Links

TARGETS	
Ion Channels[a]	**Nuclear hormone receptors**[c]
TRPV1 channels	PGC1α
Enzymes[b]	PPARα
AMPK, AMP kinase	PPARγ
CaMKII	**Transporters**[d]
SIRT-1	UCP-1

LIGANDS
BMP8b
Capsaicin
Capsazepine
FSK, forskolin

These Tables list key protein targets and ligands in this article, which are hyperlinked to corresponding entries in http://www.guidetopharmacology.org, the common portal for data from the IUPHAR/BPS Guide to PHARMACOLOGY (Southan *et al.*, 2016) and are permanently archived in the Concise Guide to PHARMACOLOGY 2015/16 ([a,b,c,d]Alexander *et al.*, 2015a,b,c,d).

Introduction

Obesity is the hallmark of metabolic syndrome (Maestu *et al.*, 2010). It foreshadows type II diabetes, dyslipidemia, vascular anomalies and the overall risk of cardiovascular diseases (Arya *et al.*, 2002). Decreased physical activity coupled with increased high-fat diet (HFD) intake prompts obesity (Yagi *et al.*, 2014). Effective clinical management is still lacking to combat obesity. Recent studies indicate that high fructose in a diet is a critical factor leading to obesity as the combination of sugars and refined carbohydrates along with fat lead to metabolic syndrome (DiNicolantonio *et al.*, 2015; Lucan and DiNicolantonio, 2015). Recent evidence suggests that browning of white adipose tissue (WAT) might serve as a novel strategy to improve metabolic health (Bartelt and Heeren, 2014). WAT stores energy in the form of fat, while brown adipocytes promote energy expenditure via thermogenesis by burning fat. Browning of WAT favours the energy expenditure by triggering thermogenesis, which suppresses diet-induced weight gain (Cao *et al.*, 2011; Bordicchia *et al.*, 2012; Bi *et al.*, 2014). Further analysis of molecular mechanisms underscoring induction of browning of WAT led to identification of adipogenic factors, their stabilization and interaction with proteins, which serve as catalysts for browning of WAT (Ohno *et al.*, 2012; Qiang *et al.*, 2012; Cohen *et al.*, 2014). Harnessing brown fat thermogenesis has opened new strategies to counteract obesity (Peschechera and Eckel, 2013; Vosselman *et al.*, 2013; Wu *et al.*, 2013).

Obesity is associated with decreased thermogenesis. Browning of WAT involves the expression and activation of the brown fat-specific genes in white adipocytes (Lu *et al.*, 2012; Lo and Sun, 2013; Rosell *et al.*, 2014; Servera *et al.*, 2014). Bone morphogenetic proteins regulate thermogenesis and fatty acid oxidation (Molliver *et al.*, 2005 Futamura *et al.*, 2009; Tramontana *et al.*, 2009). Bone morphogenetic protein 8b (BMP8b) facilitates energy dissipation by thermogenesis (Whittle *et al.*, 2012). Another important protein that regulates brown fat thermogenesis is uncoupling protein 1 [UCP-1; (Hesselink *et al.*, 2003)]. UCP-1 is localized on the inner mitochondrial membrane and it short-circuits the mitochondrial proton gradient to promote thermogenesis. Mice lacking UCP-1 are also prone to obesity at thermoneutrality (Melnyk and Himms-Hagen, 1998; Denjean *et al.*, 1999).

Recognition of a role for PRDM-16, a transcriptional co-regulator that controls the development of brown adipocyte genes (Ohno *et al.*, 2012; Lo and Sun, 2013) and deacetylation of PPARγ by sirtuin 1 (SIRT-1), a cellular energy sensor (Qiang *et al.*, 2012), have prompted a search for ways to promote SIRT-1-mediated stabilization of the PRDM-16/PPARγ protein complex. This induces browning of WAT, a change emerging as a new strategy to treat obesity.

SIRT-1, a central player that regulates the browning program in WAT, is a sensor of cellular metabolism and energy utilization. SIRT-1 is phosphorylated and activated by cellular protein kinases including Ca^{2+}/calmodulin-dependent protein kinase kinase β (Iwabu *et al.*, 2010), AMP-activated protein kinase (AMPK; Peng *et al.*, 2010; Passariello *et al.*, 2011; Lau *et al.*, 2014). Also, intracellular Ca^{2+}-dependent Ca^{2+}/calmodulin-activated protein kinase (CaMKII)-AMPK signalling has been implicated in metabolism and fatty acid oxidation, where CaMKII has been recognized as an upstream regulator of AMPK (Raney and Turcotte, 1985). Thus, assessment of the crosstalk signalling between intracellular Ca^{2+}-activated CaMKII-AMPK signalling and subsequent activation of SIRT-1 are essential for the regulation of browning of WAT.

Previous research has revealed a role for the TRPV1 ion channels in the pathogenesis of metabolic disorders (Zhang *et al.*, 2007; Motter and Ahern, 2008; Kang *et al.*, 2010; Yu *et al.*, 2012; Marshall *et al.*, 2013). Capsaicin, an agonist of TRPV1 channels, in the diet prevented HFD-induced obesity and loss of TRPV1 channels prevented obesity (Cui and Himms-Hagen, 1992; Motter and Ahern, 2008). Here, we analyzed the effects of dietary capsaicin (0.01%) on HFD (60% kcal from fat)-induced obesity in wild-type (WT) mice and $TRPV1^{-/-}$ mice (that genetically lack TRPV1 channels).

This study evaluated the effects of feeding mice a 60 kcal% HFD and water *ad libitum*. From a nutritional perspective, a diet of 60 kcal% fat may be considered as extreme. Nonetheless, a HFD with 60 kcal% fat is commonly used to induce obesity in mice because they tend to become obese within a short period of time (Johnston *et al.*, 2007). This permits us to screen the effects of dietary capsaicin and its ability to prevent obesity. Also, it is important to note that if dietary capsaicin can counter obesity induced by feeding HFD with 60 kcal% fat, it should be effective in countering obesity in humans who consume comparable or even less fat-containing diets. In contrast, a

previous research study has used omega-3 fatty acids containing HFD in obesity research to evaluate the effects of TRPV1 channels. The results of that study suggest that lack of TRPV1 channels prevented obesity (Motter and Ahern, 2008). However, this observation could result from the beneficial effects of omega-3 fatty acids containing HFD or use of a lower fat-containing diet along with omega-3 (Motter and Ahern, 2008). Consistently, published work suggests that those mice fed diets containing fish oil did not gain as much weight as those fed diets with more saturated fat (Ikemoto *et al.*, 1996). Also, in this study, we show for the first time a novel mechanism by which dietary capsaicin stimulated browning of WAT. Capsaicin stimulated SIRT-1 by activating CaMKII/AMPK-dependent phosphorylation of SIRT-1. This triggered the deacetylation and interaction of proteins to mediate browning of WAT in mouse model.

Our data show that mammalian epididymal fat (EF) and subcutaneous fat pads from the inguinal region (SCF), expressed TRPV1 channel protein endogenously, and HFD suppressed expression of TRPV1 channels in these adipose tissues. The findings reported in this article show the potential of dietary capsaicin to cause browning of WAT. Our findings should contribute towards developing a novel strategy to counter obesity in humans.

Methods

Mouse model of HFD-induced obesity

All animal care and experimental procedures were approved by the University of Wyoming Institutional Animal Care and Use Committee. Animal studies are reported in compliance with the ARRIVE guidelines (Kilkenny *et al.*, 2010; McGrath and Lilley, 2015). Adult male WT and TRPV1$^{-/-}$ (B6.129X1-*Trpv1*^{tm1Jul}/J) mice purchased from Jackson Laboratory, Maine, USA, were housed in the research animal facility and maintained at 23°C at the School of Pharmacy, University of Wyoming. Mice were housed in groups of four and proper husbandry care was exercised according to the recommendations of the Institutional Animal Care and Use Committee of the University of Wyoming. Mice were allowed access to the different diets and water *ad libitum*.

General procedures. Mice are routinely used in studies to determine the molecular mechanisms underlying diet-induced obesity, adipogenesis and thermogenesis. The data obtained through mouse model of obesity have the translational potential for human interventions. Experimental animals (n = 40 per group) were randomly assigned and housed in groups of four in separate cages. Their weekly weight gain and food/water intake were recorded for analysis. The weights and all other *in vivo* and *in vitro* data in this study were obtained and their analyses carried out, without the knowledge of the treatment groups (blinded).

Experimental procedures. All mice were fed a normal diet for the first six weeks. Starting from week 6, WT and TRPV1$^{-/-}$ mice were randomly assigned into four groups and fed with the four different diets – normal chow diet (NCD), NCD with added capsaicin (0.01%; NCD+CAP), the high fat diet (HFD; 60 kcal% fat; http://www.researchdiets.com/opensource-diets/stock-diets/dio-series-diets) or HFD with added capsaicin (0.01%; HFD +CAP). These diets were fed till week 32. The average weight gain and food/water intake were determined on a weekly basis. At the end of 32 weeks, a metabolic study was performed with a group of mice that were fed NCD, HFD or HFD + CAP. Epididymal and subcutaneous fats were obtained at the end of 32 weeks of feeding and used for quantitative RT-PCR and Western blotting. Primers that were used for RT-PCR experiments are given in Table 1.

Quantitative RT-PCR measurements

EF and SCF pads were collected from groups of four mice from the different diet groups and pooled for experiments. Each experiment was performed in duplicate for statistical analysis. Total RNA was isolated using Tri Reagent (Sigma, USA) according to manufacturer's instructions, and cDNA was synthesized using Quantitect reverse transcription kit (Qiagen, Valencia, CA) using Q5plex PCR system (Qiagen). Real-time PCR was performed using Quantitect SYBR green PCR kit on Q5plex system. 18s mRNA was used as the reference gene. Amplification was performed using 20 μL reaction volume according to the manufacturer's instruction.

Table 1

Primers (IDT, USA) that were used for RT-PCR experiments

Genes	Forward	Reverse
18 s	ACC GCA GCT AGG AAT AAT GGA	GCC TCA GTT CCG AAA ACC A
gapdh	CGT GCC GCC TGG AGA AAC C	TGG AAG AGT GGG AGT TGC TGT TG
mtrpv1	CAA CAA GAA GGG GCT TAC ACC	TCT GGA GAA TGT AGG CCA AGA C
pparα	GTA CCA CTA CGG AGT TCA CGC AT	CGC CGA AAG AAG CCC TTA C
pparγ	CAA GAA TAC CAA AGT GCG ATC AA	GAG CAG GGT CTT TTC AGA ATA ATA AG
sirt-1	TCG TGG AGA CAT TTT TAA TCA GG	GCT TCA TGA TGG CAA GTG G
prdm-16	CAG CAC GGT GAA GCC ATT C	GCG TGC ATC CGC TTG TG
bmp8b	TCC ACC AAC CAC GCC ACT AT	CAG TAG GCA CAC AGC ACA CCT
ucp-1	CGA CTC AGT CCA AGA GTA CTT CTC TTC	GCC GGC TGA GAT CTT GTT TC
pgc-1α	AGA GAG GCA GAA GCA GAA AGC AAT	ATT CTG TCC GCG TTG TGT CAG G

Table 2

Sources of antibodies used in the experiments

Antibodies	Source	Catalog no.
PPARα	Novus Biologicals, USA	NB600-636
PPARγ	Santa Cruz Biotechnology, Inc., USA	SC-7273
PRDM-16	Novus Biologicals, USA	NBP1-77096
BMP-8b	Santa Cruz Biotechnology, Inc., USA	SC-13086
SIRT-1	Santa Cruz Biotechnology, Inc., USA	SC-28766
UCP-1	Santa Cruz Biotechnology, Inc., USA	SC28766
TRPV1	Santa Cruz Biotechnology, Inc., USA	SC-28759
β-actin	Santa Cruz Biotechnology, Inc., USA	SC47778
Acetylated lysine	Cell Signaling Inc., USA	9441
CaMKIIα	Santa Cruz Biotechnology, Inc., USA	SC-5306
AMPKα	Cell Signaling Inc., USA	2532S
Phospho-CaMKIIα	Santa Cruz Biotechnology, Inc., USA	SC-12886-R
Phospho-AMPKα	Cell Signaling Inc., USA	2535S
Phosphoserine	Santa Cruz Biotechnology, Inc., USA	SC-81516
Phosphothreonine	Santa Cruz Biotechnology, Inc., USA	SC-9386
GAPDH	Santa Cruz Biotechnology, Inc., USA	SC-365062

Immunoblotting

EF and SCF pads were washed with chilled PBS and homogenized in lysis buffer (50 mM Tris pH 7.5, 250 mM sodium chloride, 0.5% NP40, 0.5% sodium deoxycholate, 2 mM EDTA, 0.5 mM dithiothreitol, 1 mM sodium orthovanadate and protease inhibitor cocktail) and centrifuged at 20 817× *g* for 20 min to remove tissue debris. The protein concentration was determined using Bradford method, and equal amounts of protein were separated by SDS-PAGE, transferred to nitrocellulose membrane and immunoblotted with specific antibodies. Sources of antibodies are shown in Table 2.

Co-immunoprecipitation

Protein was precleared using protein A/G agarose beads and incubated with non-immune serum or rabbit polyclonal anti-acetylated lysine antibody or monoclonal PPARγ or polyclonal TRPV1 antibody overnight at 4°C. Then protein A/G agarose beads were added and incubated for 2 h at 4°C. Beads were pelleted by centrifugation and washed three times with lysis buffer and eluted in 1% SDS buffer, resolved on 10% SDS-PAGE and analyzed by immunoblotting with PPARγ, TRPV1 or PRDM-16 antibodies.

Isolation and primary culture of EF and SCF preadipocytes

The EF or SCF pads were isolated from mice at the end of 32 weeks of feeding the different diets and minced in 500 μL ice-cold sterile PBS. Collagenase (0.5mL of 1.5 mg·mL^{-1}) in isolation buffer (123 mM NaCl, 5 mM KCl, 1.3 mM $CaCl_2$, 5 mM glucose, HEPES 100 mM, 1% penicillin and streptomycin, and 4% BSA (fraction V) were added and incubated in shaking water bath at 37°C for 45 min, with 10 s vortexing for every 5 min. The digested tissues were filtered (100 μm filter) and centrifuged at 370× *g* for 5 min. The pellet was resuspended in 1 mL of red blood cell lysis buffer for 1 min. Sterile PBS (9 mL) was added and filtered (70 μm filter). The pellet was resuspended in DMEM (high glucose) containing 20% FBS, 20 mM HEPES and 1% penicillin and streptomycin and added to 1% gelatin-coated plates for 45 min to remove the fibroblasts. The supernatant was then seeded in treated cell culture plates. The cells appeared rounded when plated and 24 h later, they adhered, elongated and had spindle-shape appearance.

Cell culture and transfection

HEK293 cells (ATCC, VA, USA) were maintained in minimal essential medium (Invitrogen, USA) supplemented with 10% FBS and 1% penicillin/streptomycin. The rat TRPV1 protein tagged with the *myc* epitope on the N terminus in pCDNA3 vector was transfected using the Effectene reagent (Qiagen, USA). Two days post-transfection, cells expressing TRPV1 protein were exposed to medium containing 1 mg·mL^{-1} G418 for 2 weeks, and cells that survived the G418 pressure were pooled to develop a stable cell line of HEK293 cells expressing TRPV1 protein (designated as HEKTRPV1) and used for immunocytochemical, intracellular Ca^{2+} imaging and Western blotting experiments.

Intracellular Ca^{2+} imaging

Preadipocytes were cultured in DMEM supplemented with 10% FBS and antibiotics. For intracellular Ca^{2+} imaging, preadipocytes or cells grown on 25 mm circular coverslips were incubated with Fura-2 AM (2 μM; for 60 min) at room temperature in an extracellular buffer containing in mM, NaCl 137, KCl 5, $CaCl_2$ 1.8, $MgCl_2$ 1. HEPES 10, glucose 10 and pH 7.38. The coverslips were then washed with buffer, placed in a stainless steel holder (0.8 mL volume) and viewed with a Leica DMI3000 B inverted microscope coupled to a Polychrome V digital imaging system equipped with Imago CCD camera. Cells were continuously superfused (22°C) with

buffer, and Ca^{2+} entry following addition of capsaicin (1 μM) in the presence of 2 mM extracellular Ca^{2+} containing buffer was measured. Results were analyzed using TillVision 5 software and presented as the ratio (*R*) of fluorescence intensities at excitation wavelengths of 340 and 380 nm collected at 510 nm. Intracellular Ca^{2+} imaging experiments, using HEK293 cells stably expressing TRPV1 channel protein, were carried out exactly as described for the experiments with preadipocytes.

Oil Red O staining of preadipocytes

Preadipocytes were washed three times with PBS and then fixed with 10% formaldehyde for 10 min. The cells were treated with propylene glycol for 2 min followed by Oil Red O in propylene glycol (0.5%) for 15 min. The Oil Red O was removed, and 60% polyethylene glycol was added for 1 min. The cells were then rinsed with water, and the nucleus was stained with haematoxylin for 10 min. The nuclear staining was intensified with sodium phosphate solution for 5 min. The coverslips were washed with water several times and mounted using aqueous mounting medium. The cells/sections were visualized under an Olympus upright microscope fitted with a SPOT-imaging camera.

Immunocytochemistry

HEKTRPV1 cells were grown on 25 mm round glass coverslips, were fixed with 2 mL of 4% paraformaldehyde in PBS at room temperature for 30 min. The cells were washed twice with PBS (2 mL) and treated with 2 mL of 100 mM glycine in PBS for 30 min. After washing with PBS twice, the cells were permeabilized with 300 μL of cold methanol at −20°C for 5 min and washed once with 2 mL PBS. The cells were then blocked with 5% goat serum for 1 h at 37°C in an incubator followed by a wash with PBS and incubation with the anti-TRPV1 antibody (1:100 dilution as specified by the manufacturer) for 6 h in cold followed by FITC antibody (1:1000) in PBS for another 1 h at 4°C. The cells were then washed three times (2 mL each) with PBS, washed once with distilled water, mounted on a glass slide with mounting media and observed with a Zeiss LSM-710 confocal microscope, equipped with an argon laser (488 nm), in the Confocal Imaging Facility of the University of Wyoming.

Measurement of metabolic activity

Metabolic activity and respiratory quotient were determined for NCD-fed, HFD-fed and HFD + CAP-fed WT and TRPV1$^{-/-}$ mice at the end of 32 weeks of feeding the respective diets by using the Comprehensive Laboratory Animal Monitoring System [CLAMS™, Columbus Instruments, Columbus, OH, USA (Ren, 2004; Turdi *et al.*, 2011)], which represents a set of live-in cages for automated, non-invasive and simultaneous monitoring of food and water consumptions, horizontal and vertical activities and metabolic performance. Mice were individually placed in the CLAMS metabolic cages with *ad libitum* access to food and water. After acclimatization for 48 h, metabolic parameters including the volume of carbon dioxide produced (VCO_2), the volume of oxygen consumed (VO_2), the respiratory exchange ratio (RER = VCO_2/VO_2), the caloric (heat) value and activity were determined. Metabolic rate was calculated by using the modified Weir equation [(Moudiou *et al.*, 2007); Metabolic rate = $(3.941 * VO_2 + 1.106 * VCO_2)/100$].

Mouse fecal fat analysis

Mouse fecal fat analysis was performed by collecting the feces of NCD-fed, HFD-fed or HFD + CAP-fed WT and TRPV1$^{-/-}$ mice. Feces were collected from both groups of mice, and the total fat from the fecal samples was extracted as previously described (Van De Kamer *et al.*, 1949; Neufeld, 1952; Jeejeebhoy *et al.*, 1970) and the extract was evaporated to dryness and weighed (Jeejeebhoy *et al.*, 1970).

Basal and forskolin-stimulated glycerol release

Inguinal fat pads were removed and washed in PBS and incubated in pre-warmed DMEM. For basal lipolysis, cut tissue pieces (approximately 20 mg) were preincubated in 200 μL of DMEM containing 2% fatty acid-free BSA at 37°C, 5% CO_2 and 95% humidified atmosphere for 60 min. The incubation medium was saved for performing lipolysis assay. For forskolin stimulation, the cut tissue pieces (approximately 20 mg) were preincubated in 200 μL DMEM containing 2% fatty acid-free BSA and 10 μM forskolin and 5 μM Triacsin C and preincubated at 37°C in 5% CO_2 and 95% humidified atmosphere for 60 min. The fat explants were transferred to identical medium and incubated for further 60 min (period of measurement) at 37°C, 5% CO_2 and 95% humidified atmosphere, and the incubation medium was saved for lipolysis assay. The fat explants were transferred into 1 mL of extraction solution [chloroform: methanol (2:1 v/v) and 1% glacial acetic acid] and incubated for 60 min at 37°C with vigorous shaking. The fat explants were transferred into 500 μL of lysis solution (0.3 N NaOH containing 0.1% SDS) and incubated overnight at 55°C with vigorous shaking, and the protein concentration was determined using BCA reagent and BSA as standard. Glycerol content of the incubation medium was determined using free glycerol reagent and extrapolating the unknown sample values from the standard curve plotted using glycerol standards. Lipolysis of inguinal fat culture was calculated as glycerol release in nmol per mg of protein per h (Schweiger *et al.*, 2014).

Glycerol release assay from preadipocytes

Preadipocytes were prepared from 0.5 g of inguinal fat pads after killing the mice fed the different diets for 32 weeks. The culture medium was collected after 24 h after plating the cells and was frozen until analyzed. The cells were washed twice with PBS and lysed using lysis buffer (50 mM Tris pH 7.5, 250 mM sodium chloride, 0.5% NP40, 0.5% sodium deoxycholate, 2 mM EDTA, 0.5 mM dithiothreitol, 1 mM sodium orthovanadate and protease inhibitor cocktail), and protein content of cell lysate was determined. Samples (40 μg) of these cell lysates were separated by 15% polyacrylamide SDS-PAGE, transferred to nitrocellulose membrane and immunoblotted for anti FABP4-marker for preadipocytes and GAPDH for loading control, which further confirmed the viability of the preadipocytes. The glycerol released by the preadipocytes into the cell culture medium was determined as an index of lipolysis as described previously (Arner and Langin, 2014). Briefly, to a vial of free glycerol reagent (Sigma Aldrich, St. Louis, MO), sterile deionized water (40 mL) was added and mixed several times by inversion. Amplex Ultra Red® (Invitrogen, Carlsbad, CA) 1 mg was reconstituted in dark with 340 μL of DMSO to get a 10 mM solution and was

stored protected from light. Amplex UltraRed® was diluted 100-fold in glycerol reagent, and 180 μL was added per well in a 96-well plate. The blank value was determined by adding 20 μL of complete medium used for the culture of preadipocytes. Medium(20 μL) from preadipocytes obtained from NCD-fed or HFD (±CAP)-fed WT and TRPV1$^{-/-}$ mice was added and mixed for 10 s using an orbital shaker and incubated in the dark for 15 min. The fluorescence intensity was measured (Ex530/Em590) using a TECAN Infinite M200 plate reader. Quadruplicate measurements were performed for each sample, and mean ± SEM of glycerol release, as nmol·per mg of protein per h, was calculated after normalizing to the blank value.

Data and statistical analyses

The study design and analysis conformed to the recent guidance on experimental design and analysis (Curtis *et al.*, 2015). Data are expressed as mean ± SEM. Student *t*-test and ANOVA evaluated the statistical significance of population means. $P < 0.05$ was deemed to constitute the threshold for statistical significance for data comparison. *Post hoc* analyses were carried out only when the means are significant for $P < 0.05$, and there was no significant variance in homogeneity. Graphs from analyzed data were plotted using Microcal Origin 6.0 software.

Materials

HFD was obtained from Research Diets Inc., NJ, USA. All chemicals were obtained from Sigma, USA. Quantitative RT-PCR kits were obtained from Qiagen, USA.

Results

Effect of dietary capsaicin on HFD-induced obesity

Weekly body weight gain, food intake and water intake were monitored for NCD (±CAP)-fed and HFD (±CAP)-fed TRPV1$^{-/-}$ mice and their genetically unaltered WT controls. The mean values body weight, food or water consumption for NCD (± CAP)-fed or HFD (±CAP)-fed WT and TRPV1$^{-/-}$ mice are given in Table 3.

Figure 1A illustrates the picture of NCD-fed WT and HFD (± CAP)-fed WT and TRPV1$^{-/-}$ mice at the end of 32 weeks of feeding the respective diet. Dietary capsaicin suppressed HFD-induced weight gain but did not suppress weight gain in NCD-fed mice. Aversion to capsaicin-containing diets (possible because capsaicin is a major component of chilli peppers) was not observed in either WT or TRPV1$^{-/-}$ mice. The food and water intake was not altered by dietary capsaicin in either NCD-fed or HFD-fed animals.

Effect of HFD on expression of TRPV1 protein

HFD caused obesity in WT and TRPV1$^{-/-}$ mice, and dietary capsaicin protected only WT but not TRPV1$^{-/-}$ mice. To determine the effect of HFD on TRPV1 protein expression, we evaluated the endogenous expression of this protein in the EF and SCF fat pads of WT and TRPV1$^{-/-}$ mice-fed NCD or HFD (± CAP). We immunoprecipitated TRPV1 protein in the lysates obtained from these fat pads. HEKTRPV1 and control HEK293 cells (these cells did not express TRPV1 protein endogenously) were used as positive and negative controls respectively. Figure 1B shows the expression of TRPV1 protein in these cells and in the EF and SCF of WT mice. The quantification of TRPV1 mRNA in EF and SCF is given in Figure 1C and D. TRPV1 protein immunoprecipitation in EF and SCF is shown in Figure 1E, and the quantification of band intensity is given in Figure 1F. HFD suppressed the expression of TRPV1 protein in both EF and SCF, and CAP antagonized this effect. No expression of TRPV1 protein was observed in the EF and SCF of TRPV1$^{-/-}$ mice.

Effect of dietary capsaicin on respiratory quotient, heat production and locomotor activity of HFD-fed WT but not TRPV1$^{-/-}$ mice

Because dietary capsaicin significantly antagonized HFD-induced obesity, we analyzed the effect of this addition on the metabolic activity of mice by using CLAMS™. We determined the respiratory quotient (RER), heat production and ambulatory activity of NCD-fed, HFD-fed or HFD + CAP-fed WT and TRPV1$^{-/-}$ mice. As shown in Figure 2, dietary capsaicin stimulated heat production (Figure 2A–C) and

Table 3

Body weight and food and water intake in NCD or HFD (±CAP)-fed wild type and TRPV1$^{-/-}$ mice

	WT				TRPV1$^{-/-}$			
Group	**NCD**	**NCD + CAP**	**HFD**	**HFD + CAP**	**NCD**	**NCD + CAP**	**HFD**	**HFD + CAP**
Weight (g) in week 6	18.55 ± 1.1	19.51 ± 0.97	18.35 ± 1.01	18.54 ± 0.91	18.22 ± 0.88	18.87 ± 1.15	19.11 ± 0.94	18.14 ± 1.03
Weight (g) in week 38	29.70 ± 1.30	28.90 ± 1.19	50.33 ± 1.33	32.12 ± 0.98	29.04 ± 1.22	30.33 ± 0.95	49.34 ± 1.55	48.33 ± 1.68
Number of mice	40	20	40	40	40	20	40	40
Food intake (g·day^{-1} per mouse)	3.52 ± 0.61	3.35 ± 0.8	3.22 ± 0.71	3.18 ± 0.81	3.44 ± 0.76	3.53 ± 0.54	3.13 ± 0.38	3.20 ± 0.70
Water intake (mL·day^{-1} per mouse)	4.92 ± 0.93	4.88 ± 0.82	3.96 ± 1.22	4.02 ± 0.66	5.11 ± 1.06	4.86 ± 0.85	4.04 ± 1.02	3.98 ± 1.14

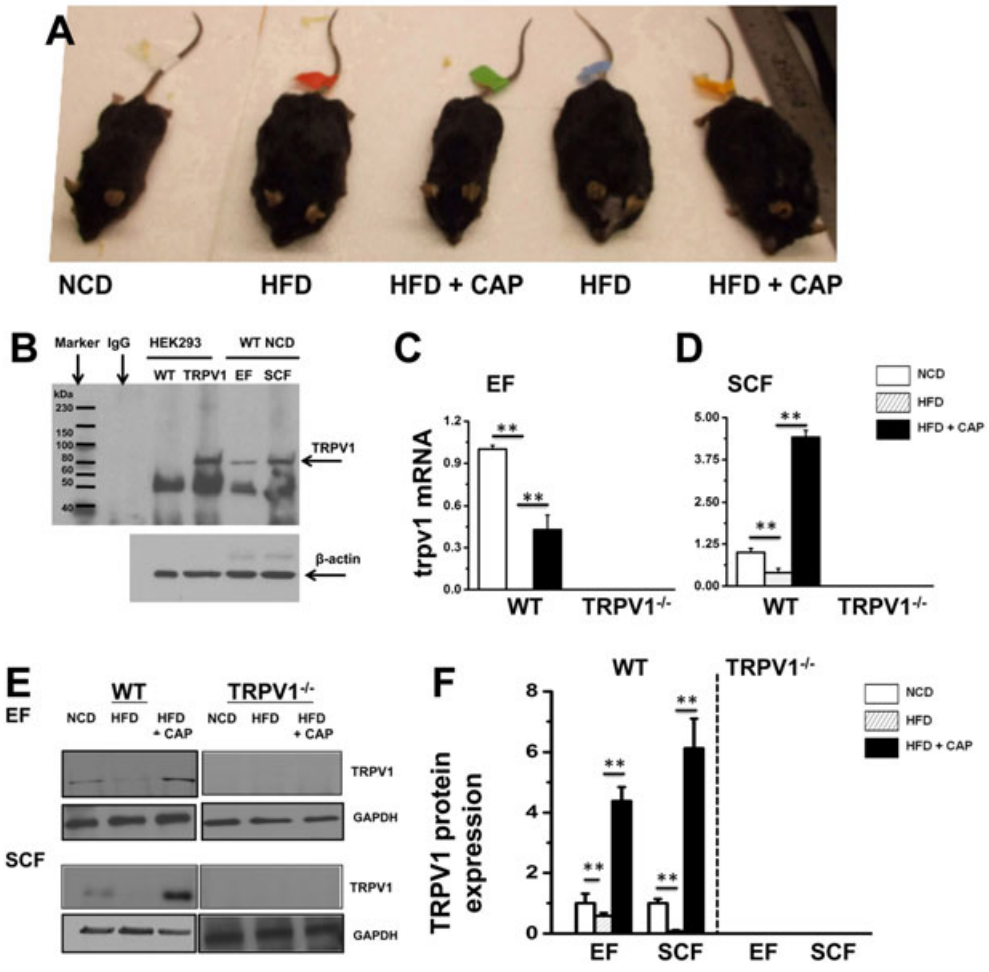

Figure 1

Dietary capsaicin prevents obesity in WT but not in TRPV1$^{-/-}$ mice and counters the suppressive effect of HFD on TRPV1 expression. (A) Representative images of WT and TRPV1$^{-/-}$ mice fed with respective dietary regimen (n = 40). (B) Representative Western blots showing the expression of TRPV1 channel protein in HEK293 WT, HEK-TRPV1 cells, EF and SCF isolated from NCD-fed WT and TRPV1$^{-/-}$ mice at 38 weeks of age. (C) and (D) The average mRNA levels ± SEM of *trpv1* normalized to NCD in EF and SCF. 18s ribosomal RNA was used as control. (E) TRPV1 expression in EF and SCF pads of NCD-fed and HFD (± CAP)-fed WT mice and TRPV1$^{-/-}$ conditions. (F) Ratios of band intensity ± SEM of TRPV1 to GAPDH (loading control); data shown are means ± SEM. ** $P < 0.05$, significantly different as indicated.

increased RER (Figure 2D–F) in WT mice, while both RER and heat production remained decreased in HFD-fed WT and HFD (± CAP)-fed TRPV1$^{-/-}$ mice. Also, HFD significantly decreased the locomotor and ambulatory activity of WT and TRPV1$^{-/-}$ mice, and dietary capsaicin stimulated higher activity only in the WT mice (Figure 2G).

In order to evaluate whether dietary capsaicin altered the assimilation of fat and increased the excretion of fat in the feces, which lead to a decrease in fat absorption, we measured fecal fat excreted by NCD-fed or HFD (± CAP)-fed WT and TRPV1$^{-/-}$ mice by gravimetric analysis. The fat excreted in 10 g of feces collected from eight mice per condition was analyzed and shown in Figure 2H.

HFD suppresses TRPV1 channel activity

The protective effect of dietary capsaicin on HFD-induced obesity and stimulation of metabolic activity suggest that the activity of TRPV1 channels is important. Therefore, we analyzed TRPV1 channel activity by measuring capsaicin (1 μM)-stimulated Ca^{2+} influx in primary epididymal and subcutaneous preadipocytes isolated from NCD-fed or HFD (± CAP)-fed WT and TRPV1$^{-/-}$ mice. The changes in Fura-2 AM fluorescence ratio (F340/380) were measured before and after stimulating with capsaicin *in vitro*. The results are illustrated in Figure 3. capsaicin-stimulated Ca^{2+} entry was not observed in the preadipocytes isolated from HFD-fed mice (Figure 3B and H), while capsaicin-stimulated Ca^{2+} influx was observed in preadipocytes isolated from both NCD-fed and HFD + CAP-fed WT mice (Figure 3C and I). The ratio of change in fluorescence intensity between the baseline and peak is summarized in Figure 3F for primary preadipocytes isolated from EF. Capsaicin did not stimulate a Ca^{2+} influx in the preadipocytes of TRPV$^{-/-}$ mice (Figure 3D, E and J–L). The ratio of change in fluorescence intensity between the baseline and peak is summarized in Figure 3M for SCF preadipocytes.

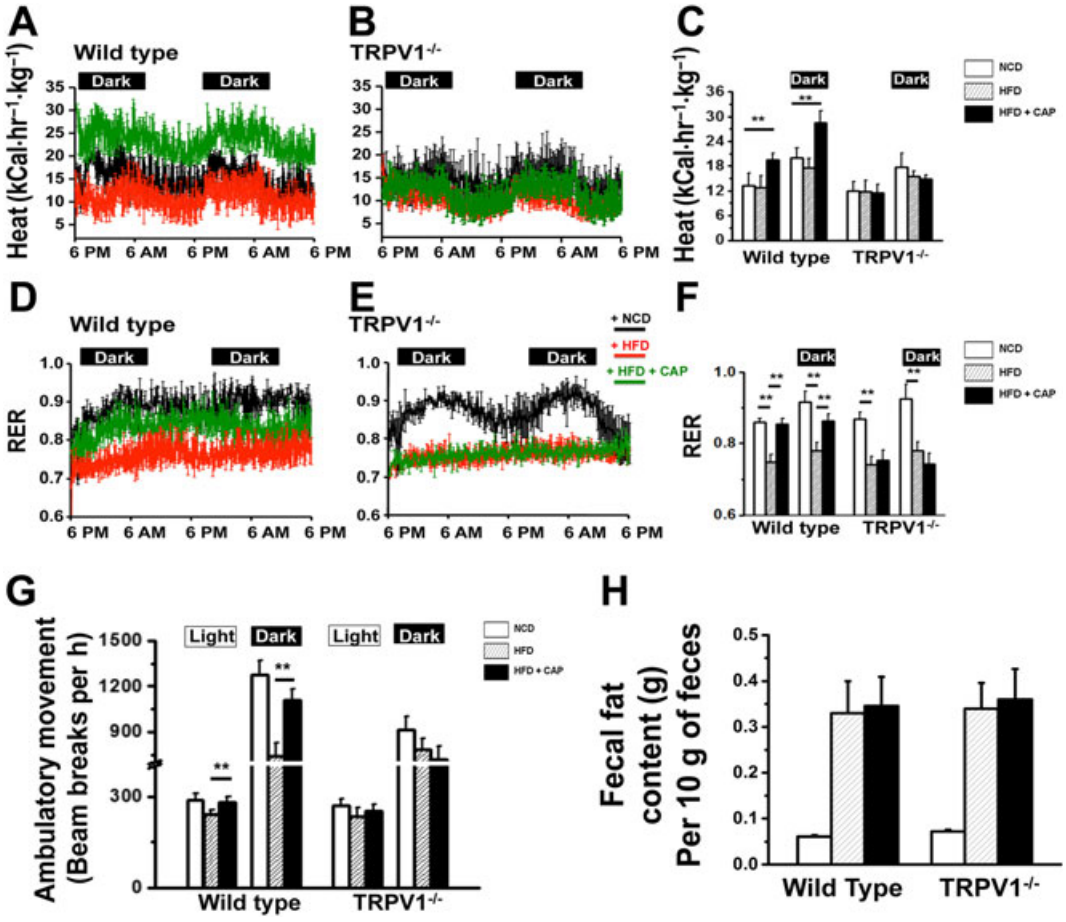

Figure 2

Dietary capsaicin increases metabolic activity. (A) and (B) Representative traces of time course of heat production (in kCal·hr^{-1}·kg^{-1}) during the dark and light cycles in NCD-fed, HFD-fed or HFD + CAP-fed WT and TRPV1$^{-/-}$ mice ($n = 40$) calculated by using the modified Weir equation [Metabolic rate (heat production) = (3.941 * VO_2 + 1.106 * VCO_2)/100]. (D) and (E) Representative traces of time course of RER [ratio of carbon dioxide production (VCO_2) to oxygen consumption (VO_2)] measured by CLAMS, during the dark and light cycles for NCD-fed, HFD-fed or HFD + CAP-fed WT and TRPV1$^{-/-}$ mice. Respiratory quotient (RER) and heat production were calculated from the values of VCO_2 and VO_2. (C) and (F) Mean ± SEM heat production and RER during the dark and light cycles for NCD-fed, HFD-fed or HFD + CAP-fed WT and TRPV1$^{-/-}$ mice; ** $P < 0.05$; significantly different as indicated. (G) Beam breaks per hour (means ± SEM) for the same groups of mice during the dark and light cycles. (I) Dietary capsaicin did not alter fat assimilation: bar graphs represent mean fat ± SEM excreted per 10 g of feces. Samples were obtained from NCD-fed or HFD (± CAP)-fed WT and TRPV1$^{-/-}$ mice.

Dietary capsaicin decreases lipid content in primary preadipocytes

HFD increased lipid content in the fat pads. Therefore, we wanted to examine whether capsaicin feeding decreases lipid content in the preadipocytes isolated from the fat pads. We performed Oil Red O staining of epididymal and subcutaneous preadipocytes to examine their lipid content. Figure 4 shows the Oil Red O staining for the preadipocytes from EF (Figure 4A, panels 1–3) and SCF (Figure 4B, panels 4–6) isolated from NCD-fed or HFD (±CAP)-fed WT and TRPV1$^{-/-}$ mice. The bottom panel for each condition gives the images at a higher magnification. Lower magnification image of Oil Red O staining of SCF adipocytes is shown in Supporting Information Fig. S1A. Dietary capsaicin significantly decreased lipid content in the preadipocytes of WT but not TRPV1$^{-/-}$ mice. Fibroblast contamination is a common problem in adipocyte cultures. In order to confirm that we isolated preadipocytes for our experiments, we analyzed the expression of the adipocyte progenitor (preadipocyte) marker FABP4 (Shan *et al.*, 2013) in the preadipocyte lysates and a Western blot for FABP4 is shown in Supporting Information Fig. S1D. Supporting Information Fig. S1E represents the quantification for FABP4 protein expression.

Dietary capsaicin increases adipogenic transcriptional PPARs in EF and SCF

PPARs regulate metabolic homeostasis. PPARγ plays a cardinal role in adipocyte gene expression and differentiation, while PPARα regulates lipid metabolism and promotes fatty acid oxidation. In order to understand the effect of CAP on the expression of PPARs, we measured the mRNA and

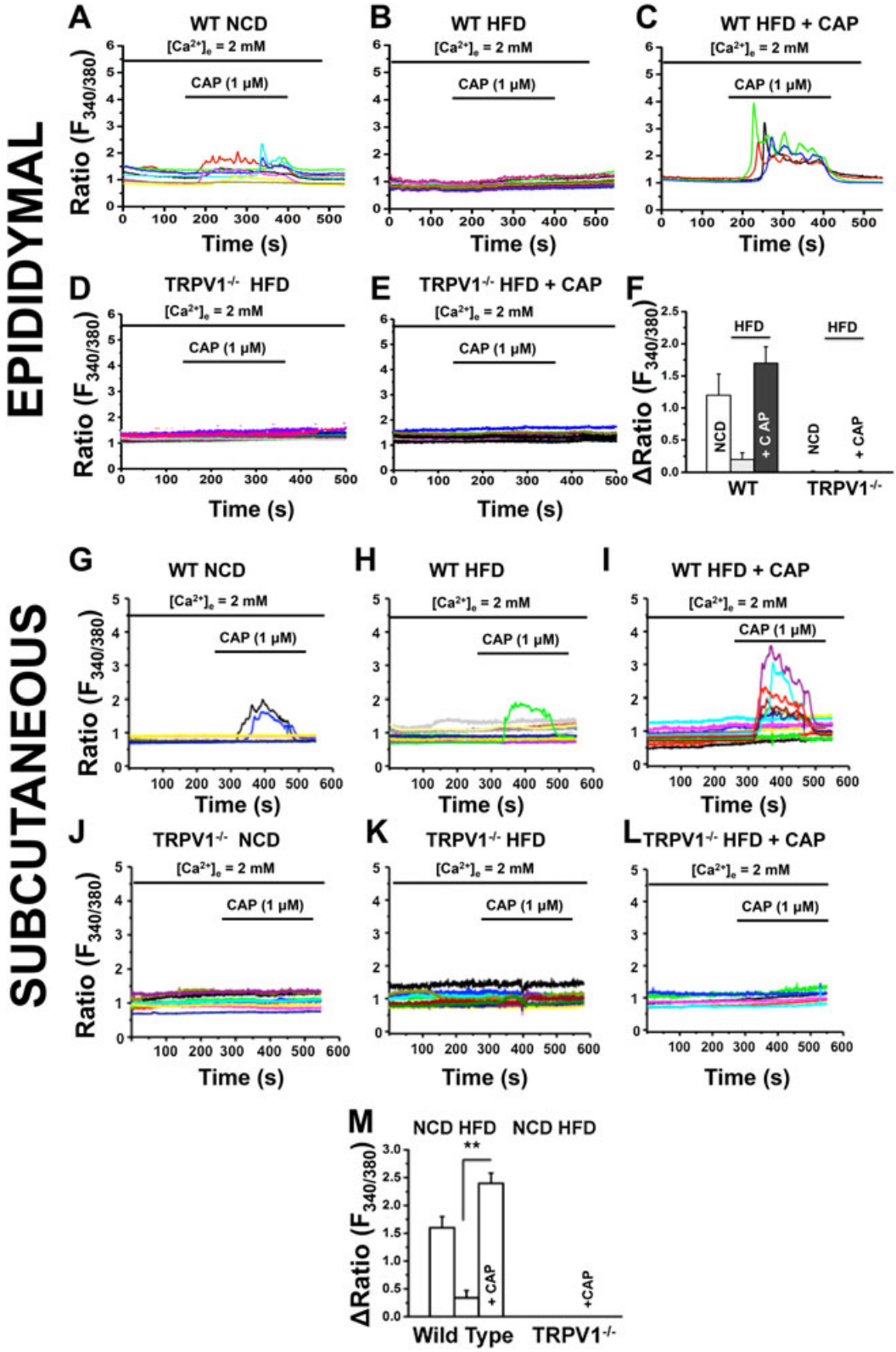

Figure 3

HFD suppresses TRPV1 channel activity in epididymal and subcutaneous preadipocytes, and dietary capsaicin antagonizes this. Representative traces of time courses of capsaicin-stimulated (1 μM) Ca^{2+} influx measured in Fura-2 AM loaded primary epididymal and subcutaneous preadipocytes obtained from NCD-fed, HFD-fed or HFD + CAP-fed WT [EF: A–C; SCF: G–I] $TRPV1^{-/-}$ [EF: D and E; SCF: J–L]. (F) The average change in fluorescence ratio after the addition of 1 μM CAP ± SEM is given for epididymal and subcutaneous preadipocytes of WT and $TRPV1^{-/-}$ mice ($n = 40$) under each condition and used for the imaging experiments. ** $P < 0.05$; significantly different as indicated.

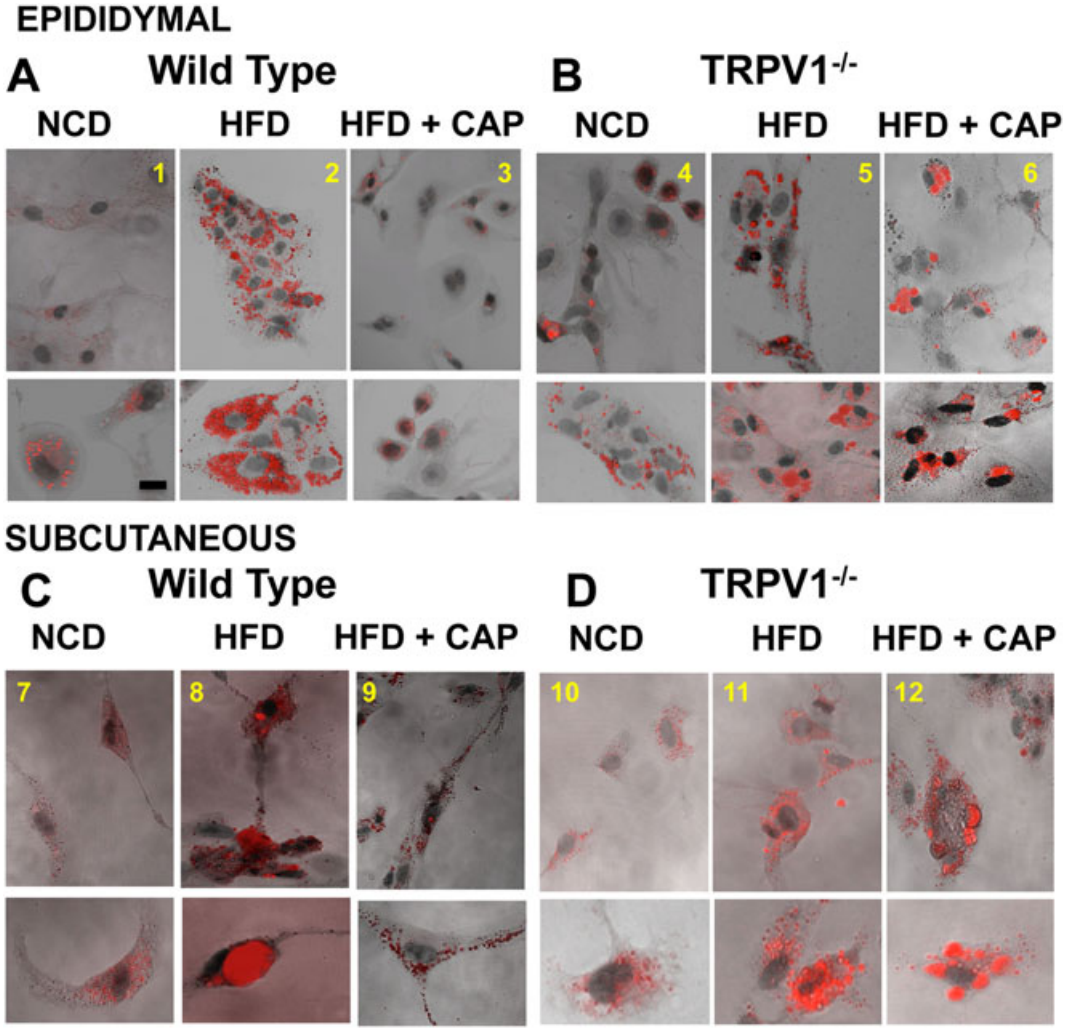

Figure 4

HFD promotes lipid content in epididymal and subcutaneous preadipocytes, and dietary capsaicin counters this. Preadipocytes were isolated at the end of 32 weeks of feeding respective diets, and lipid droplets in preadipocytes were estimated using Oil Red O staining. Representative micrographs of epididymal and subcutaneous (inguinal) preadipocytes isolated from NCD-fed, HFD-fed or HFD + CAP-fed WT (A, panels 1–3 and C, panels 7–9) and TRPV1$^{-/-}$ (B, panels 4–6 and D, panels 10–12) mice (n = 40).

protein levels of PPARs in EF and SCF isolated from WT and TRPV1$^{-/-}$ mice-fed NCD or HFD (± CAP). HFD decreased the expression of PPARα, which was counter-regulated by dietary capsaicin. However, PPARγ was increased in fat pads from both HFD and HFD + CAP mice, particularly in the SCF. The mRNA and protein expression of PPARα and PPARγ are given in Figure 5A, B, D and E. Figure 5C summarizes the mean ± SEM of the PPARs protein quantification in EF and SCF.

Dietary capsaicin increases lipolysis in SCF

Lipolysis is a catabolic process, which breaks down triglycerides stored in fat cells, releasing fatty acids and glycerol. PPARα activation has been shown to increase the breakdown of lipids into fatty acids and glycerol (Guzman *et al.*, 2004). In our model, dietary capsaicin increased PPARα in SCF and significantly decreased the lipid content of the SCF preadipocytes. This result might reflect the increased breakdown of lipids in these cells. Therefore, we evaluated the effect of dietary capsaicin on glycerol release in SCF preadipocytes obtained from HFD-fed WT and TRPV1$^{-/-}$ mice. Mean glycerol release ± SEM per mg of protein from SCF is given in Supporting Information Fig. S1B. We also evaluated the basal and forskolin-stimulated glycerol release in the inguinal fat pads isolated from these mice (Supporting Information Fig. S1C). Forskolin stimulates PKA-induced lipolysis (Yehuda-Shnaidman *et al.*, 2010) and enhanced glycerol release in inguinal WAT. The basal as well as forskolin-stimulated lipolysis was higher in SCF from mice given dietary capsaicin.

Dietary capsaicin increases the brown adipocyte-specific thermogenic genes in WAT

The phenomenon of browning of WAT is associated with an increase in the expression of the brown fat-specific

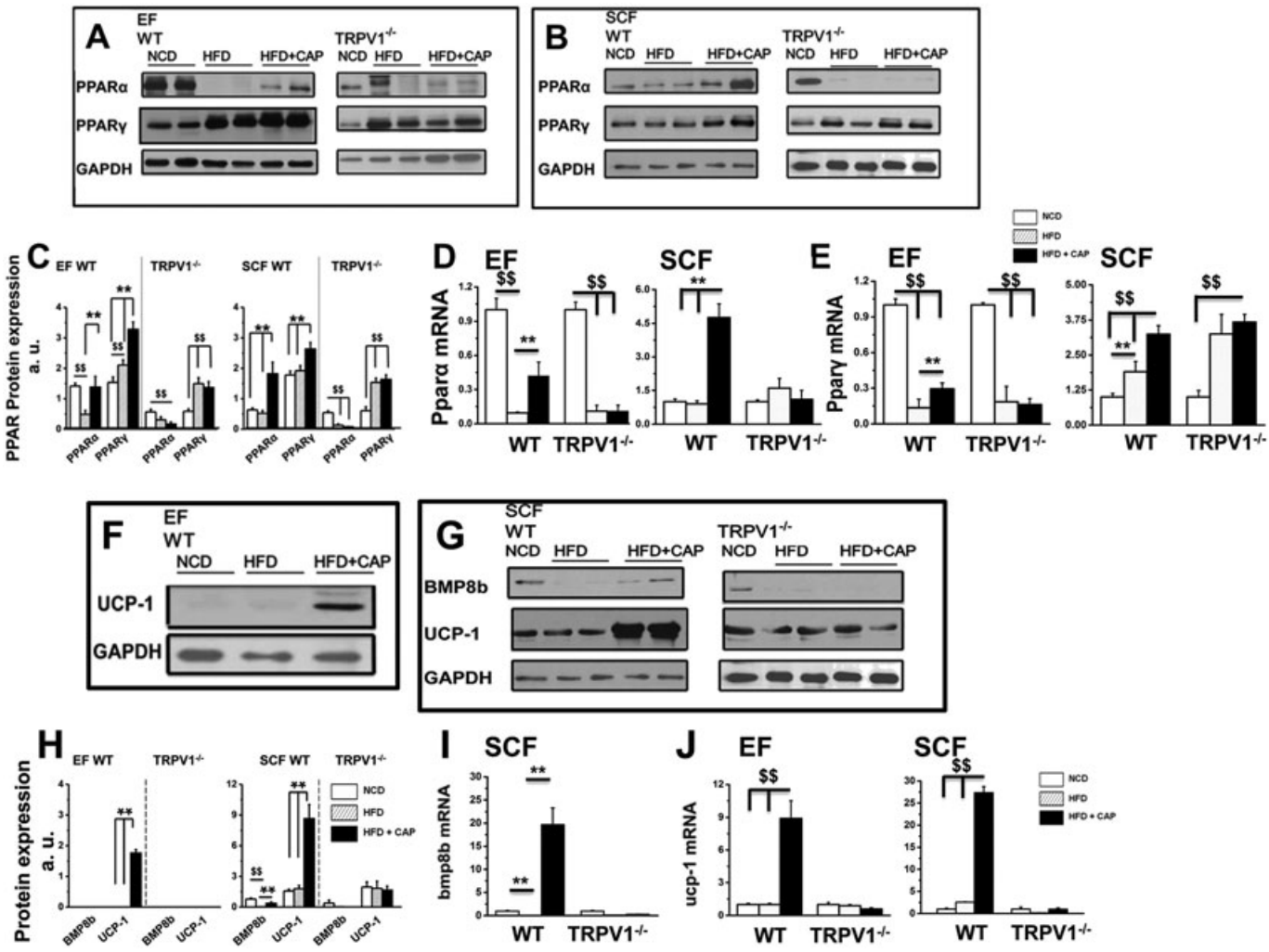

Figure 5

Dietary capsaicin increases PPARs and brown fat-specific genes/proteins in WAT of WT but not TRPV1$^{-/-}$ mice. (A), (B), (F) and (G) PPARα, PPARγ BMP8b and UCP-1expression in EF and SCF obtained from NCD-fed, HFD-fed or HFD + CAP-fed WT (left panel) and TRPV1$^{-/-}$ mice following 32-weeks of feeding respective diets. (C) and (H) Ratio of PPARs, BMP8b and UCP-1 expression in EF and SCF normalized to GAPDH (loading control). The average mRNA levels ± SEM of *pparα* (D), *pparγ* (E), *bmp8b* (I) and *ucp-1* (J) normalized to NCD in EF and SCF are given for NCD-fed, HFD-fed or HFD + CAP-fed WT and TRPV1$^{-/-}$ mice. For quantitative RT-PCR experiments, 18s ribosomal RNA was used as control ($n = 40$). $$ and ** $P < 0.05$; significantly different as indicated.

thermogenic genes/proteins in WAT (Shabalina *et al.*, 2013). Previous research also indicates that activating and stabilizing PPARγ may promote browning of WAT. Because adding dietary capsaicin increased PPARγ in EF and SCF of WT mice compared with those fed with HFD alone, we asked whether this enhanced expression of PPARγ is associated with an increase in brown fat-specific thermogenic genes/proteins that induce browning of WAT.

We therefore analyzed the mRNA and protein levels of mitochondrial UCP-1 and BMP8b in EF and SCF of WT and TRPV1$^{-/-}$ mice. The protein expression of UCP-1 and BMP8b in EF and SCF is shown in Figure 5F and G. UCP-1 was not detected in the EF of WT and TRPV1$^{-/-}$ mice, but dietary capsaicin markedly induced the expression of UCP-1 in EF (Figure 5 F). No expression of BMP8b was detected in the EF of WT and TRPV1$^{-/-}$ mice. The protein intensities for all conditions are summarized in Figure 5H. We also quantified the mRNA expression for *bmpb8* (Figure 5I) and *ucp-1* (Figure 5J) in EF and SCF of WT and TRPV1$^{-/-}$ mice.

Next, we measured the expression of *pgc-1α* (encoding PPARγ coactivator-1α), a key regulator of cellular energy and metabolism. *pgc-1α* participates in driving up the mRNA as well as protein expression of UCP-1 to increase energy expenditure (Kong *et al.*, 2014). The mRNA levels of *pgc-1α* in the EF and SCF are given in Figure 6A and B. Dietary capsaicin significantly increased *pgc-1α* mRNA in both the fat pads of WT mice. These data suggest that dietary capsaicin could increase metabolic activity and energy utilization by up-regulating *pgc-1α*, which stimulates *ucp-1*-dependent mechanism. The induction of UCP-1 in EF and overall increase in UCP-1 and BMP8b in SCF suggests that CAP may trigger browning phenomenon in WAT to produce brown in white (brite) cells.

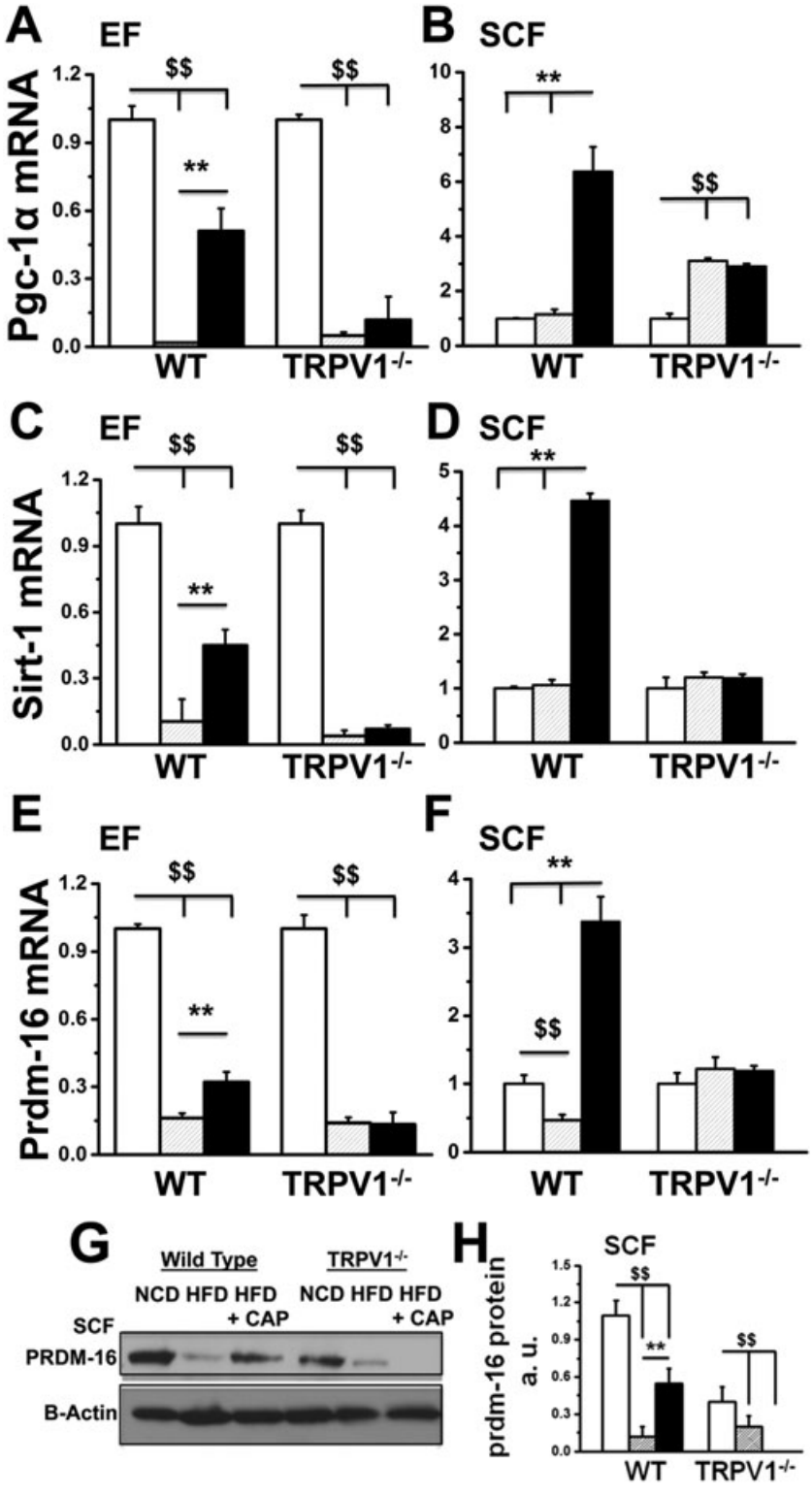

Figure 6

Dietary capsaicin increases the expression of *pgc-1α*, *sirt-1* and *prdm-16* in EF and SCF of WT but not TRPV1$^{-/-}$ mice. The average mRNA levels ± SEM of *pgc-1α*, *sirt-1* and *prdm-16* normalized to NCD in EF (A, C and E) and SCF (B, D and F) are given for NCD-fed, HFD-fed or HFD + CAP-fed WT and TRPV1$^{-/-}$ mice (n = 40). (G) Representative Western blot for PRDM-16 expression in SCF of WT and TRPV1$^{-/-}$ mice. (H) Ratio of mean band intensity ± SEM between PRDM-16 and β-actin. $$ and ** $P < 0.05$; significantly different as indicated.

Dietary capsaicin increases the expression of genes that trigger the molecular conversion of white to brite cells

Browning of WAT is a molecular process that is triggered by the expression and activity of *sirt-1* (encoding a NAD^+-dependent deacetylase) and *prdm-16* (encoding a transcriptional co-regulator for browning of WAT). Thus, by increasing the expression of *sirt-1* and *prdm-16*, dietary capsaicin could induce the molecular conversion of WAT to brite cells. We therefore measured the mRNA levels of *sirt-1* and *prdm-16* normalized to 18s, in the EF and SCF (Figure 6C–F). The expression of PRDM-16 is shown in Figure 6G, and the quantification of PRDM-16 protein is given in Figure 6H. HFD-suppressed *prdm-16* expression and dietary capsaicin antagonized this effect. SIRT-1 deacetylates and stabilizes PPARγ, which triggers the browning program in WAT (Qiang *et al.*, 2012). Therefore, it is important to evaluate whether dietary capsaicin caused stabilization of PPARγ through SIRT-1. We performed the following experiments in SCF isolated from NCD-fed or HFD (± CAP)-fed WT and $TRPV1^{-/-}$ mice.

Dietary capsaicin causes SIRT-1-dependent deacetylation of PPARγ and PRDM-16 and facilitates PPARγ–PRDM-16 interaction

Previous evidences illustrate that post-translational modifications of PPARγ, including sumoylation, acetylation, phosphorylation and ubiquitination, differentially regulate its adipogenic functions (van Beekum *et al.*, 2009; Anbalagan *et al.*, 2012; Qiang *et al.*, 2012). Acetylation of PPARγ by the inhibition of histone deacetylase increases its transcriptional activity and adipogenesis (Jiang *et al.*, 2014). It is well known that PRDM-16 is a determinant of brown adipocyte lineage, which causes browning of WAT (Seale *et al.*, 2008). Further, deacetylation of PPARγ by SIRT-1 stabilizes PPARγ and facilitates its interaction with PRDM-16 to trigger browning of WAT (Qiang *et al.*, 2012; Tian *et al.*, 2014). Therefore, we evaluated the acetylation status of PPARγ and PRDM-16 in SCF of NCD-fed, HFD-fed or HFD + CAP-fed mice and also determined PPARγ–PRDM-16 interaction by co-immunoprecipitation (Co-IP) technique. The expression levels of PPARγ and PRDM-16 in the input are given in Figure 7A, and the acetylated lysine levels of these proteins in the immunoprecipitates are given in Figure 7B. We determined the acetylated states of PPARγ and PRDM-16 using acetylated lysine antibody. The ratios of acetylated PPARγ to PPARγ and acetylated PRDM-16 to PRDM-16 are given in Figure 7C and D respectively. Interactions between PRDM-16 and PPARγ were assessed by Co-IP experiments using extracts of SCF from WT and $TRPV1^{-/-}$ mice. As shown in Figure 7E and F, we immunoblotted PPARγ in 10% precleared SCF lysate (Figure 7E) of NCD-fed, HFD-fed or HFD + CAP-fed WT and $TRPV1^{-/-}$ mice. Figure 7F shows an interaction between PRDM-16 and PPARγ in SCF, after immunoprecipitation of PPARγ in these samples. Together, our data illustrate a novel TRPV1-dependent mechanism by which dietary capsaicin increased the interaction between PPARγ and PRDM-16 to trigger browning of WAT.

Dietary capsaicin causes CaMKIIα/AMPKα-dependent SIRT-1 phosphorylation and activation

Next, we evaluated how TRPV1 channel activation by capsaicin promotes SIRT-1 phosphorylation and activation to facilitate PPARγ/PRDM-16 interaction, which causes browning of WAT. Activation of TRPV1 increases intracellular Ca^{2+}, which activates Ca^{2+}-dependent protein kinases. CaMKIIα is activated by such an intracellular Ca^{2+} rise (Larrucea *et al.*, 2008; Zhang *et al.*, 2011). Also, CaMKIIα activation leads to AMPK activation (Raney and Turcotte, 1985), which phosphorylates and activates SIRT-1 (Draznin *et al.*, 2012). Therefore, we determined the effects of activation of TRPV1 channels by CAP on the expression and phosphorylation of CaMKII, AMPK and SIRT-1 in the SCF of NCD-fed or HFD (± CAP)-fed WT and $TRPV1^{-/-}$ mice (Figure 8A, 8B). Figure 8C and D show the expression of SIRT-1 and phospho-SIRT-1 in SCF of NCD-fed or HFD (CAP)-fed WT and $TRPV1^{-/-}$ mice. HFD significantly suppressed the levels of phospho-CaMKII [Thr^{286} (Zhou *et al.*, 2012)] and phospho-AMPK [Thr^{172} (Shen *et al.*, 2007; Pulinilkunnil *et al.*, 2011)], and dietary capsaicin prevented this in the SCF of WT but not $TRPV1^{-/-}$ mice. Also, dietary capsaicin increased the expression of SIRT-1 and its phosphorylation, suggesting its plausible effect on SIRT-1 activation.

We also analyzed the expression of these proteins in HEK293 cells that stably expressed TRPV1 channel proteins (HEKTRPV1 cells). Figure 9A and B shows the expression of TRPV1 protein in HEKTRPV1 cells, but not in WT HEK293 cells. Figure 9C shows the effects of intracellular Ca^{2+} chelation by BAPTA-AM or TRPV1 channel blockade by capsazepine, on capsaicin (1 μM)-stimulated Ca^{2+} influx in HEKTRPV1 cells. Both capsazepine and BAPTA-AM significantly suppressed capsaicin-stimulated Ca^{2+} influx in HEKTRPV1 cells. Figure 9D shows the change in intracellular Ca^{2+} following the addition of capsaicin in untreated (control), capsazepine or BAPTA-AM pretreated HEKTRPV1 cells.

The expression of CaMKII, phospho-CaMKII, AMPK and phospho-AMPK in the control, capsaicin-treated, capsazepine-treated, BAPTA-treated or KN62-treated cells is illustrated in Figure 9E, G and H, and the ratios of phospho-CaMKII to CaMKII and phospho-AMPK to AMPK are given in Figure 9F and I respectively. If capsaicin mediates these effects by stimulating influx of Ca^{2+}, then inhibiting TRPV1 channels (with capsazepine) or chelating intracellular Ca^{2+} will prevent the effect of capsaicin. To evaluate this, we pre-stimulated HEKTRPV1 with either vehicle (capsaicin untreated) or capsaicin (1 μM for 30 min). Subgroups of HEKTRPV1 cells were treated with capsazepine (10 μM; 60 min and present throughout the experiment), BAPTA-AM (10 μM; cell permeable intracellular Ca^{2+} chelator; 60 min) or KN62 (5 μM; CaMKII inhibitor; 60 min) prior to treatment with capsaicin.

Capsaicin treatment significantly increased CaMKIIα phosphorylation, which was inhibited by TRPV1 channel block by capsazepine, intracellular Ca^{2+} chelation by BAPTA-AM or CaMKIIα inhibition by KN62. These data clearly suggest the involvement of raised intracellular Ca^{2+}, via activation of TRPV1 and CaMKIIα, by capsaicin in SIRT-1 phosphorylation. Consistent with these findings,

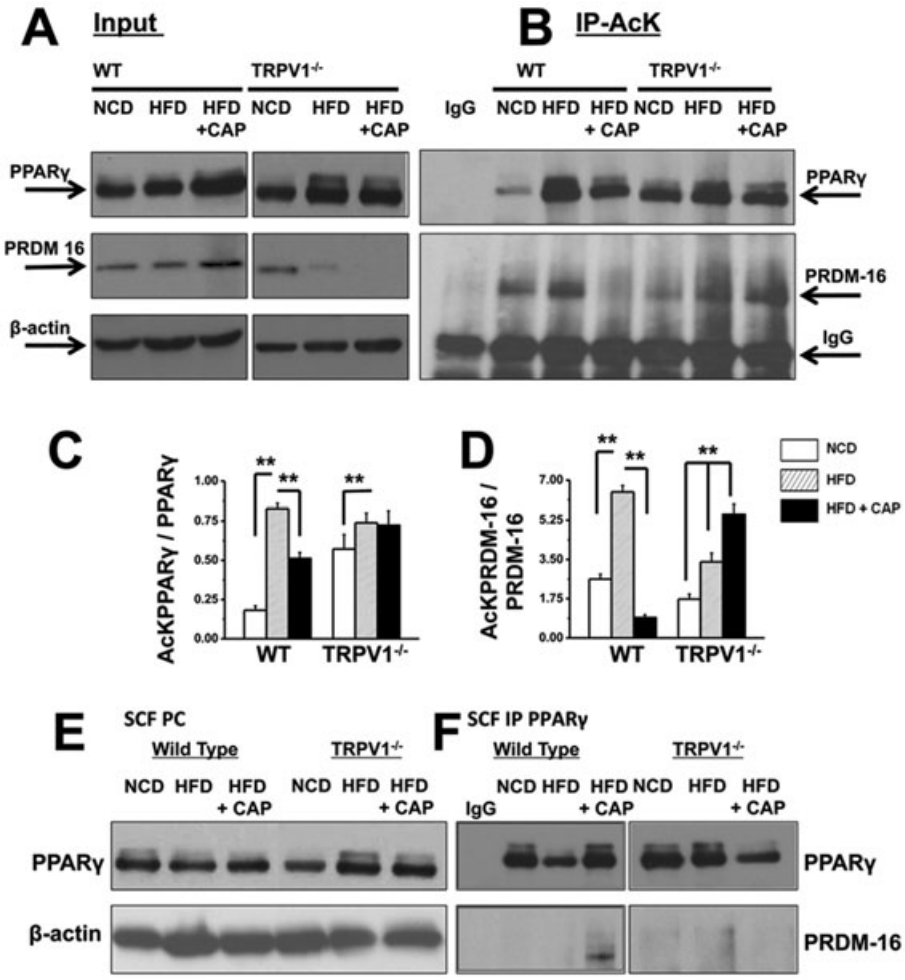

Figure 7

Dietary capsaicin decreases PPARγ and PRDM-16 acetylation and increases PRDM-16–PPARγ interaction in SCF of WT but not TRPV1$^{-/-}$ mice. SCF pads from NCD-fed, HFD-fed or HFD + CAP-fed WT and TRPV1$^{-/-}$ mice (n = 40) were lysed and immunoprecipitated with acetylated lysine (AcK) antibody and immunoblotted with PPARγ and PRDM-16 antibodies. (A) Western blots for PPARγ and PRDM-16 in 10% of total protein used for Co-IP studies. (β-actin, loading control). (B) Immunoprecipitation of samples with acetylated lysine (AcK) antibody shows acetylated PPARγ and PRDM-16. No PPARγ/PRDM-16 was pulled down by IgG, indicating the specificity of the antibodies. (C) and (D) Mean intensity ratio of acetylated PPARγ to total PPARγ ± SEM and acetylated PRDM-16 to total PRDM-16 ± SEM, respectively, for each condition. ** $P < 0.05$; significantly different as indicated; one-way ANOVA. (E) Immunoblot for PPARγ in 10% precleared (PC) lysate from SCF of NCD-fed and HFD (± CAP)-fed WT and TRPV1$^{-/-}$ mice (β-actin, loading control). (F) PPARγ immunoprecipitation showing the interaction between PRDM-16 and PPARγ in SCF.

capsaicin treatment stimulated AMPKα phosphorylation, the effect of which was inhibited by capsazepine, BAPTA-AM or KN62 (Figure 9G and H).

Phosphorylation of CaMKII and AMPK stimulates SIRT-1 phosphorylation and its activity. To evaluate this, we measured the expression and phosphorylation of SIRT-1 in HEKTRPV1 cells pretreated with capsaicin alone or with capsazepine, BAPTA-AM or KN62. SIRT-1 expression and its phosphorylation under these conditions are given in Figure 9J and K. The expression of SIRT-1 was not significantly altered under these conditions. These data suggest a TRPV1-activated increase in intracellular Ca^{2+} stimulated the CaMKII/AMPK-dependent mechanism by which capsaicin stimulates SIRT-1 activation. This resulted in the deacetylation of PPARγ and PRDM-16 as well as inducing their interaction to trigger browning of WAT to increase metabolic activity.

Discussion

Obesity is an important contributing factor for the metabolic syndrome. Identification of new molecular targets that suppress diet-induced obesity will advance the development of effective strategies to counter obesity. Recently, a role for TRPV1 activation by capsaicin has been recognized in the regulation of diet-induced obesity (Zhang *et al.*, 2007; Liu *et al.*, 2008; Yu *et al.*, 2012). This work systematically analyzed the mechanism by which activation of TRPV1 channels countered obesity using an *in vivo* mouse model and WAT isolated from obese mice. We used TRPV1$^{-/-}$ mice throughout the study as an ideal control for the TRPV1-dependent effect of capsaicin. Although previous research has reported the thermogenic effects of capsaicin, the mechanism by which this effect was exerted this still remains undefined. Interestingly,

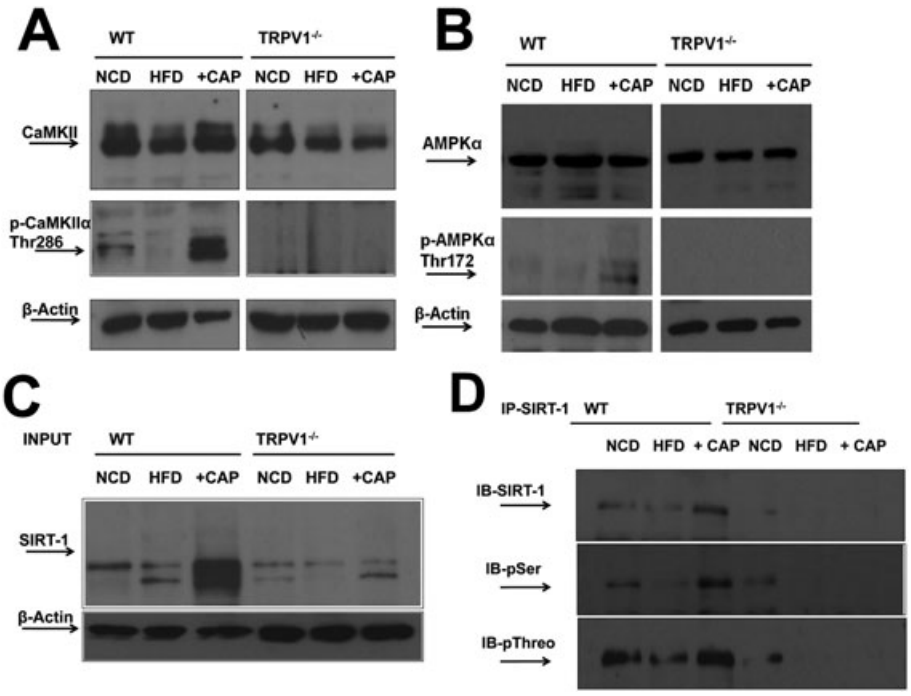

Figure 8

Dietary capsaicin activates SIRT-1 via TRPV1-CaMKIIα-AMPK-dependent mechanism. (A) and (B) Representative Western blots for the expression levels of CaMKIIα/p-CaMKIIα (Thr^{286}) and AMPKα/p-AMPKα (Thr^{172}) in 40 μg of SCF lysate (β-actin, loading control; $n = 40$). (C) and (D) Representative Western blot shows immunoprecipitation of SIRT-1 (10% input) and immunoblotting with anti-SIRT-1 antibody. (D) Representative blot showing SIRT-1 phosphorylation using phosphoserine and threonine antibodies in the immunoprecipitated samples.

recent research suggested a thermogenic effect of capsaicin in rodents and humans (Yoneshiro and Saito, 2013), which also supports the importance of TRPV1 channels in the process.

In this study, we used pure capsaicin (16 million Scoville heat units) to add to the diet fed to our mouse model. Several studies have employed capsaicinoids [capsaicin mixed with other ingredients of capsicum plant (Bloomer *et al.*, 2010; Dulloo, 2011; Luo *et al.*, 2011)], which makes it difficult to know whether the capsaicinoids contained a standardized amount of capsaicin (Al Othman *et al.*, 2011). Also, it makes the interpretation of the results less clear because of the variability in capsaicin concentrations in these preparations. Therefore, we chose to use pure capsaicin for the study.

Previous research suggests that dietary capsaicin or pepper-rich food decreased appetite (Yoshioka *et al.*, 1999; Hochkogler *et al.*, 2014; Janssens *et al.*, 2014). However, our data clearly demonstrate that mice did not show any aversion to an HFD containing capsaicin and we did not observe any changes in the food intake between NCD (± CAP)-fed or HFD (± CAP)-fed mice. One reason could be that the mice were fed capsaicin-containing diet as early as 6 weeks of age. Our data given in Table 3 unambiguously show that all mice consumed an identical quantities of the capsaicin-containing diets, regardless of the type of diet (NCD or HFD). We did not observe any appetite suppression or a decrease in energy intake in these mice.

Feeding experiments performed with the NCD + CAP diet suggest that dietary capsaicin did not prevent weight gain in NCD-fed mice (Table 3). However, dietary capsaicin did prevent weight gain induced by HFD. This suggests that dietary capsaicin did not decrease energy intake in mice. It is important to note that these experiments were performed at 23°C. The lack of experiments performed at thermoneutrality could be considered as a limitation of this work. However, it is beyond the scope of the research presented in this work.

The primary focus of this study was to analyse the effect of dietary capsaicin in WAT. Our data clearly illustrate that dietary capsaicin up-regulated the expression of protein machinery that trigger the molecular conversion of WAT to brite cells. Dietary capsaicin also significantly induced the expression of brown fat thermogenes, UCP-1 and BMP8b, a result compatible with the browning of WAT.

We also show that WAT expresses TRPV1 channels endogenously, and HFD suppressed expression of these channels. Further, our data show that dietary capsaicin prevented this suppression of TRPV1 channels in EF and SCF. This indicates that TRPV1 channel expression is important for the protective effects of dietary capsaicin. This is consistent with previous research showing that HFD caused increased weight gain in $TRPV1^{-/-}$ mice compared with WT (Lee *et al.*, 2015). Also, dietary capsaicin significantly decreased the lipid content of epididymal and inguinal preadipocytes of WT but not those of $TRPV1^{-/-}$ mice. These findings further confirm that TRPV1 channels are essential for the protective effects of dietary capsaicin.

Dietary capsaicin activated both PPARα and PPARγ in WAT (Figure 5A–E), while HFD suppressed PPARα while enhanced PPARγ expression. The increased expression of PPARα

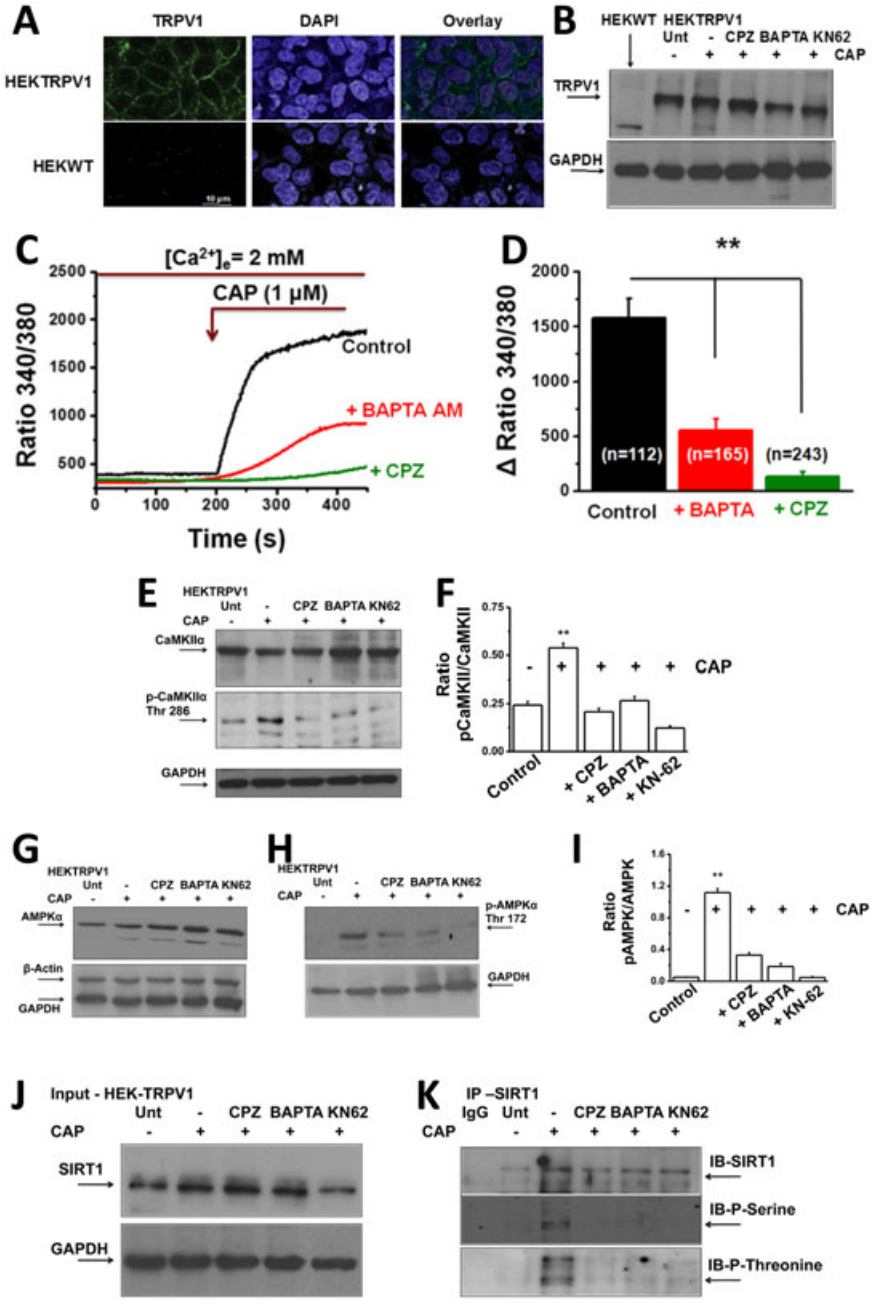

Figure 9

Intracellular Ca^{2+} chelation by BAPTA-AM or pretreatment with capsazepine (CPZ; TRPV1 antagonist) suppresses CAP-stimulated Ca^{2+} influx in HEKTRPV1 cells. (A) Left panel: TRPV1 immunoreactivity in HEKTRPV1 (top) and WT HEK293 (HEKWT) cells ($n = 6$). Middle and right panels represent DAPI staining and overlay respectively. (B) Western blot showing the expression of TRPV1 channel protein in HEKWT and HEKTRPV1 cells. Expression of TRPV1 channels in untreated cells, + capsaicin (CAP)-treated cells (1 μM; 30 min) + capsazepine (CPZ)-treated cells (10 μM; 60 min)- + 1 μM CAP-treated cells (30 min), 10 μM BAPTA-AM-treated cells (intracellular Ca^{2+} chelator; 60 min) + 1 μM CAP-treated cells or 5 μM KN62-treated cells (CaMKII inhibitor; 60 min) + 1 μM CAP-treated cells. Cells were then lysed and probed for TRPV1 expression ($n = 5$ independent experiments). (C) Representative traces showing the time courses of basal and 1 μM capsaicin-stimulated Ca^{2+} influx in HEKTRPV1 cell. These cells were pretreated with CPZ or BAPTA-AM for 60 min prior to experiments. Cells were perfused with 2 mM Ca^{2+}-containing extracellular solution, and 1 μM CAP was added as indicated by arrow in the figure. (D) Bar graphs represent average change ± SEM of Fura-2 fluorescence following 1 μM CAP stimulation in HEKTRPV1 cells pretreated with vehicle, CPZ or BAPTA-AM. Figures in parentheses represent the number of vehicle, CPZ-treated cells or BAPTA-AM-treated cells. ** represent statistical significance for $P < 0.05$. (E), (G) and (H) CaMKIIα/pCaMKIIα (Thr286) and AMPKα/pAMPKα (Thr172) expression in untreated cells (Unt; no CAP; vehicle alone; lane 1), CAP-treated cells (1 μM; 30 min; lane 2), CPZ-treated cells (10 μM; lane 3), BAPTA-AM-treated cells (10 μM; lane 4) or KN62-treated (5 μM; lane 5) HEKTRPV1 cells (GAPDH, loading control). (F) and (I) Mean ± SEM of ratio of intensities pCaMKIIα to total-CaMKIIα and pAMPKα to total AMPKα. (J) Immunoblotting of total SIRT-1 (10% input) in untreated, CAP-treated, CPZ-treated, BAPTA-AM-treated or KN62-treated HEKTRPV1 cells (GAPDH, loading control). (K) Representative Western blot showing SIRT-1 phosphorylation (using phosphoserine antibody) in the immunoprecipitated samples.

is associated with an increase in capsaicin-induced glycerol release from SCF. Dietary capsaicin enhanced basal lipolysis, and forskolin-induced lipolysis was significantly higher under CAP-fed condition compared with NCD or HFD (Supporting Information Fig. S1B and C). Although increased PPARγ expression was observed in both HFD-fed and HFD + CAP-fed mice, increased deactylation of PPARγ was observed only after the HFD + CAP diet, suggesting that dietary capsaicin stimulated PPARγ deacetylation. Dietary capsaicin also up-regulated SIRT-1 expression and phosphorylation (Figure 6C and D and Figure 8C and D). This increase in SIRT-1 was associated with a concomitant increase in the deacetylation of PPARγ and PRDM-16. Dietary capsaicin also stimulated the interaction between PPARγ and PRDM-16 (Figure 7). These data suggest that activation of SIRT-1 by capsaicin is important for these effects and are in agreement with previously published data showing a SIRT-1-dependent deacetylation of PPARγ (Qiang *et al.*, 2012) and its stabilization by interaction with PRDM-16 (Villanueva *et al.*, 2013) to cause browning of WAT. Together, the data presented in this study provide a compelling evidence for the direct involvement of TRPV1 activation in SIRT-1-dependent deacetylation of PPARγ and PRDM-16 and their interaction in WAT.

Dietary capsaicin also increased the expression of PPARγ 1 coactivator α (PGC-1α), which plays a pivotal role in cellular energy metabolism in WAT by enhancing the metabolism and energy expenditure. Activation of thermogenes in WAT should also result in increased energy expenditure and metabolic activity. Consistent with this notion, dietary capsaicin significantly enhanced the respiratory quotient and energy expenditure, which were suppressed under HFD-fed conditions (Figure 2A–G). These data are in agreement with previous research that suggests the enhancement of metabolic activity and thermogenesis (Leung, 2014; Saito, 2015) by capsaicin. Our data show that dietary capsaicin did not affect fat assimilation and did not alter the amount of fat excreted in the feces (Figure 2I). Together, these observations suggest dietary capsaicin overcomes the inhibitory effects of HFD by stimulating proteins that regulate cellular metabolism. We also show that capsaicin feeding antagonized the inhibitory effect of on ambulatory locomotor activity in the WT mice. Interestingly, under NCD-fed conditions, TRPV1$^{-/-}$ mice exhibited less locomotor activity compared with WT mice in the dark cycle (Figure 2H). This suggests that endogenous TRPV1 channels are important for basal locomotor and metabolic activity, and further studies are warranted to evaluate this.

The up-regulation of SIRT-1 and PGC-1α by dietary capsaicin was associated with an enhanced expression of thermogenic UCP-1 and BMP8b proteins in WAT of WT mice (Figure 5F–J). The brite phenotype emerges from WAT. It originates from a non-MYF5 lineage and has a positive impact on metabolism (Wu *et al.*, 2012; Keipert and Jastroch, 2014). It is important to note that differences exist between EF (visceral) and inguinal (SCF) in that the basal expression of adipogenic and thermogenic proteins is higher in SCF than in EF (Gawronska-Kozak *et al.*, 2014). The expression of thermogenic BMP8b and UCP-1 were not observed in the EF samples under control (NCD-fed) conditions, while these proteins were expressed in SCF. Dietary capsaicin induced the expression of UCP-1 but did not induce BMP8b in EF, while it increased the expression of both UCP-1 and BMP8b and induced browning of WAT. BMP8b is a brown fat thermogenic protein, and *Bmp8b*$^{-/-}$ mice show decreased metabolic rate and weight gain (Whittle *et al.*, 2012). Therefore, by increasing BMP8b protein and mRNA in SCF, dietary capsaicin induced the conversion of white to brown like phenotypes, which enhanced energy expenditure.

Capsaicin stimulated the phosphorylation of SIRT-1 by activating CaMKII and AMPK (Figure 8), and inhibition of TRPV1 or chelation of intracellular Ca^{2+} by BAPTA-AM prevented the effects of capsaicin (Figure 9E–K). Therefore, Ca^{2+} influx via TRPV1 in WAT is necessary for the activation of CaMKII and AMPK and SIRT-1 phosphorylation. Both BAPTA-AM and capsazepine decreased capsaicin-stimulated Ca^{2+} influx in these cells. This is consistent with previous work showing the requirement of intracellular Ca^{2+} rise for the activation of Ca^{2+}/calmodulin-dependent protein kinase kinase β, AMPK and SIRT-1 (Iwabu *et al.*, 2010).

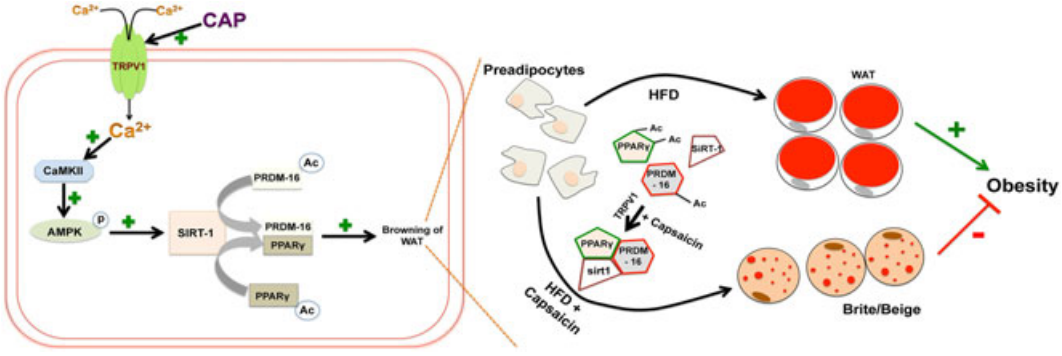

Figure 10

Model describing the mechanism of action of capsaicin (CAP). Intracellular Ca^{2+} rise via TRPV1 channels stimulated by CAP activates CaMKII/AMPK, which phosphorylate and activate SIRT-1. This causes deacetylation of PPARγ and PRDM-16 and facilitates their interaction to promote browning of WAT.

Collectively, our data demonstrate that dietary capsaicin could trigger the browning of WAT, which may be the mechanism by which dietary capsaicin counters HFD-induced obesity. Our data revealed that the 32-week chronic activation of TRPV1 channels using dietary capsaicin did not show any deleterious effects in mice. The lack of effect of dietary capsaicin in fat pads of TRPV1$^{-/-}$ mice (Figure 8A–D) suggests a central role of TRPV1 protein in browning of WAT. Our data also provide strong evidence for a novel role for the activation of TRPV1 channels in the browning program of WAT (model shown in Figure 10). It is noteworthy that future work is warranted to evaluate the effect of TRPV1 channel agonists as potential anti-obesity agents in humans. These data contribute to the development of a novel strategy to combat obesity by activating TRPV1 channels.

Acknowledgements

This work was supported by the pilot project funding from the AHA Southwest Affiliate Faculty Beginning Grant in Aid award no. 15BGIA23250030, the National Institute of General Medical Sciences of the NIH under award number 8P20 GM103432-12 and Wyoming NASA Faculty Research Initiation Grant for B.T. We thank Dr Kurt Dolence, PhD, Associate Professor, and Dr Guanglong He, PhD, Assistant Professor, School of Pharmacy for critically reading through the manuscript.

Author contributions

P.B. designed experiments, performed experiments, analyzed results and wrote the manuscript. V.K. performed experiments. J.R. performed the interpretation and analyses of results. B.T. conceived the concepts, designed experiments, performed experiments, analyzed results and wrote the manuscript.

Conflict of interest

The authors declare no conflicts of interest.

Declaration of transparency and scientific rigour

This Declaration acknowledges that this paper adheres to the principles for transparent reporting and scientific rigour of preclinical research recommended by funding agencies, publishers and other organisations engaged with supporting research.

References

Al Othman ZA, Ahmed YB, Habila MA, Ghafar AA (2011). Determination of capsaicin and dihydrocapsaicin in Capsicum fruit samples using high performance liquid chromatography. Molecules 16: 8919–8929.

Alexander SPH, Catterall WA, Kelly E, Marrion N, Peters JA, Benson HE *et al.* (2015a). The Concise Guide to PHARMACOLOGY 2015/16: Voltage-gated ion channels. Br J Pharmacol 172: 5904–5941.

Alexander SPH, Fabbro D, Kelly E, Marrion N, Peters JA, Benson HE *et al.* (2015b). The Concise Guide to PHARMACOLOGY 2015/16: Enzymes. Br J Pharmacol 172: 6024–6109.

Alexander SPH, Cidlowski JA, Kelly E, Marrion N, Peters JA, Benson HE *et al.* (2015c). The Concise Guide to PHARMACOLOGY 2015/16: Nuclear hormone receptors. Br J Pharmacol 172: 5956–5978.

Alexander SPH, Kelly E, Marrion N, Peters JA, Benson HE, Faccenda E *et al.* (2015d). The Concise Guide to PHARMACOLOGY 2015/16: Transporters. Br J Pharmacol 172: 6110–6202.

Anbalagan M, Huderson B, Murphy L, Rowan BG (2012). Post-translational modifications of nuclear receptors and human disease. Nucl Recept Signal 10: e001.

Arner P, Langin D (2014). Lipolysis in lipid turnover, cancer cachexia, and obesity-induced insulin resistance. Trends Endocrinol Metab 25: 255–262.

Arya R, Duggirala R, Almasy L, Rainwater DL, Mahaney MC, Cole S *et al.* (2002). Linkage of high-density lipoprotein-cholesterol concentrations to a locus on chromosome 9p in Mexican Americans. Nat Genet 30: 102–105.

Bartelt A, Heeren J (2014). Adipose tissue browning and metabolic health. Nat Rev Endocrinol 10: 24–36.

Bi P, Shan T, Liu W, Yue F, Yang X, Liang XR *et al.* (2014). Inhibition of Notch signaling promotes browning of white adipose tissue and ameliorates obesity. Nat Med 20: 911–918.

Bloomer RJ, Canale RE, Shastri S, Suvarnapathki S (2010). Effect of oral intake of capsaicinoid beadlets on catecholamine secretion and blood markers of lipolysis in healthy adults: a randomized, placebo controlled, double-blind, cross-over study. Lipids Health Dis 9: 72.

Bordicchia M, Liu D, Amri EZ, Ailhaud G, Dessi-Fulgheri P, Zhang C *et al.* (2012). Cardiac natriuretic peptides act via p38 MAPK to induce the brown fat thermogenic program in mouse and human adipocytes. J Clin Invest 122: 1022–1036.

Cao L, Choi EY, Liu X, Martin A, Wang C, Xu X *et al.* (2011). White to brown fat phenotypic switch induced by genetic and environmental activation of a hypothalamic-adipocyte axis. Cell Metab 14: 324–338.

Cohen P, Levy JD, Zhang Y, Frontini A, Kolodin DP, Svensson KJ *et al.* (2014). Ablation of PRDM16 and beige adipose causes metabolic dysfunction and a subcutaneous to visceral fat switch. Cell 156: 304–316.

Cui J, Himms-Hagen J (1992). Long-term decrease in body fat and in brown adipose tissue in capsaicin-desensitized rats. Am J Physiol 262: R568–R573.

Curtis MJ, Bond RA, Spina D, Ahluwalia A, Alexander SP, Giembycz MA *et al.* (2015). Experimental design and analysis and their reporting: new guidance for publication in BJP. Br J Pharmacol 172: 3461–3471.

Denjean F, Lachuer J, Geloen A, Cohen-Adad F, Moulin C, Barre H *et al.* (1999). Differential regulation of uncoupling protein-1, −2 and −3 gene expression by sympathetic innervation in brown adipose tissue of thermoneutral or cold-exposed rats. FEBS Lett 444: 181–185.

DiNicolantonio JJ, O'Keefe JH, Lucan SC (2015). Added fructose: a principal driver of type 2 diabetes mellitus and its consequences. Mayo Clin Proc 90: 372–381.

Draznin B, Wang C, Adochio R, Leitner JW, Cornier MA (2012). Effect of dietary macronutrient composition on AMPK and SIRT1 expression and activity in human skeletal muscle. Horm Metab Res 44: 650–655.

Dulloo AG (2011). The search for compounds that stimulate thermogenesis in obesity management: from pharmaceuticals to functional food ingredients. Obes Rev 12: 866–883.

Futamura M, Goto S, Kimura R, Kimoto I, Miyake M, Ito K *et al.* (2009). Differential effects of topically applied formalin and aromatic compounds on neurogenic-mediated microvascular leakage in rat skin. Toxicology 255: 100–106.

Gawronska-Kozak B, Staszkiewicz J, Gimble JM, Kirk-Ballard H (2014). Recruitment of fat cell precursors during high fat diet in C57BL/6J mice is fat depot specific. Obesity (Silver Spring) 22: 1091–1102.

Guzman M, Lo Verme J, Fu J, Oveisi F, Blazquez C, Piomelli D (2004). Oleoylethanolamide stimulates lipolysis by activating the nuclear receptor peroxisome proliferator-activated receptor alpha (PPAR-alpha). J Biol Chem 279: 27849–27854.

Hesselink MK, Mensink M, Schrauwen P (2003). Human uncoupling protein-3 and obesity: an update. Obes Res 11: 1429–1443.

Hochkogler CM, Rohm B, Hojdar K, Pignitter M, Widder S, Ley JP *et al.* (2014). The capsaicin analog nonivamide decreases total energy intake from a standardized breakfast and enhances plasma serotonin levels in moderately overweight men after administered in an oral glucose tolerance test: a randomized, crossover trial. Mol Nutr Food Res 58: 1282–1290.

Ikemoto S, Takahashi M, Tsunoda N, Maruyama K, Itakura H, Ezaki O (1996). High-fat diet-induced hyperglycemia and obesity in mice: differential effects of dietary oils. Metabolism 45: 1539–1546.

Iwabu M, Yamauchi T, Okada-Iwabu M, Sato K, Nakagawa T, Funata M *et al.* (2010). Adiponectin and AdipoR1 regulate PGC-1alpha and mitochondria by Ca(2+) and AMPK/SIRT1. Nature 464: 1313–1319.

Janssens PL, Hursel R, Westerterp-Plantenga MS (2014). Capsaicin increases sensation of fullness in energy balance, and decreases desire to eat after dinner in negative energy balance. Appetite 77: 44–49.

Jeejeebhoy KN, Ahmad S, Kozak G (1970). Determination of fecal fats containing both medium and long chain triglycerides and fatty acids. Clin Biochem 3: 157–163.

Jiang X, Ye X, Guo W, Lu H, Gao Z (2014). Inhibition of HDAC3 promotes ligand-independent PPARgamma activation by protein acetylation. J Mol Endocrinol 53: 191–200.

Johnston SL, Souter DM, Tolkamp BJ, Gordon IJ, Illius AW, Kyriazakis I *et al.* (2007). Intake compensates for resting metabolic rate variation in female C57BL/6J mice fed high-fat diets. Obesity (Silver Spring) 15: 600–606.

Kang JH, Goto T, Han IS, Kawada T, Kim YM, Yu R (2010). Dietary capsaicin reduces obesity-induced insulin resistance and hepatic steatosis in obese mice fed a high-fat diet. Obesity (Silver Spring) 18: 780–787.

Keipert S, Jastroch M (2014). Brite/beige fat and UCP1 – is it thermogenesis? Biochim Biophys Acta 1837: 1075–1082.

Kilkenny C, Browne W, Cuthill IC, Emerson M, Altman DG (2010). NC3Rs Reporting Guidelines Working Group. Br J Pharmacol 160: 1577–1579.

Kong X, Banks A, Liu T, Kazak L, Rao RR, Cohen P *et al.* (2014). IRF4 is a key thermogenic transcriptional partner of PGC-1alpha. Cell 158: 69–83.

Larrucea C, Castro P, Sepulveda FJ, Wandersleben G, Roa J, Aguayo LG (2008). Sustained increase of Ca+2 oscillations after chronic TRPV1 receptor activation with capsaicin in cultured spinal neurons. Brain Res 1218: 70–76.

Lau AW, Liu P, Inuzuka H, Gao D (2014). SIRT1 phosphorylation by AMP-activated protein kinase regulates p53 acetylation. Am J Cancer Res 4: 245–255.

Lee E, Jung DY, Kim JH, Patel PR, Hu X, Lee Y*et al.* (2015). Transient receptor potential vanilloid type-1 channel regulates diet-induced obesity, insulin resistance, and leptin resistance. FASEB J 29: 3182–3192.

Leung FW (2014). Capsaicin as an anti-obesity drug. Prog Drug Res 68: 171–179.

Liu D, Zhu Z, Tepel M (2008). The role of transient receptor potential channels in metabolic syndrome. Hypertens Res 31: 1989–1995.

Lo KA, Sun L (2013). Turning WAT into BAT: a review on regulators controlling the browning of white adipocytes. Biosci Rep 33. doi: 10.1042/BSR20130046

Lu X, Ji Y, Zhang L, Zhang Y, Zhang S, An Y*et al.* (2012). Resistance to obesity by repression of VEGF gene expression through induction of brown-like adipocyte differentiation. Endocrinology 153: 3123–3132.

Lucan SC, DiNicolantonio JJ (2015). How calorie-focused thinking about obesity and related diseases may mislead and harm public health. An alternative. Public Health Nutr 18: 571–581.

Luo XJ, Peng J, Li YJ (2011). Recent advances in the study on capsaicinoids and capsinoids. Eur J Pharmacol 650: 1–7.

Maestu J, Jurimae J, Jurimae T (2010). Visfatin and adiponectin levels in children: relationships with physical activity and metabolic parameters. Med Sport Sci 55: 56–68.

Marshall NJ, Liang L, Bodkin J, Dessapt-Baradez C, Nandi M, Collot-Teixeira S *et al.* (2013). A role for TRPV1 in influencing the onset of cardiovascular disease in obesity. Hypertension 61: 246–252.

McGrath JC, Lilley E (2015). Implementing guidelines on reporting research using animals (ARRIVE etc.): new requirements for publication in BJP. Br J Pharmacol 172: 3189–3193.

Melnyk A, Himms-Hagen J (1998). Temperature-dependent feeding: lack of role for leptin and defect in brown adipose tissue-ablated obese mice. Am J Physiol 274: R1131–R1135.

Molliver DC, Immke DC, Fierro L, Pare M, Rice FL, McCleskey EW (2005). ASIC3, an acid-sensing ion channel, is expressed in metaboreceptive sensory neurons. Mol Pain 1: 35.

Motter AL, Ahern GP (2008). TRPV1-null mice are protected from diet-induced obesity. FEBS Lett 582: 2257–2262.

Moudiou T, Galli-Tsinopoulou A, Vamvakoudis E, Nousia-Arvanitakis S (2007). Resting energy expenditure in cystic fibrosis as an indicator of disease severity. J Cyst Fibros 6: 131–136.

Neufeld OE (1952). A rapid method for determining faecal fat. J Clin Pathol 5: 288–289.

Ohno H, Shinoda K, Spiegelman BM, Kajimura S (2012). PPARgamma agonists induce a white-to-brown fat conversion through stabilization of PRDM16 protein. Cell Metab 15: 395–404.

Passariello CL, Zini M, Nassi PA, Pignatti C, Stefanelli C (2011). Upregulation of SIRT1 deacetylase in phenylephrine-treated cardiomyoblasts. Biochem Biophys Res Commun 407: 512–516.

Peng Y, Rideout DA, Rakita SS, Gower WR Jr, You M, Murr MM (2010). Does LKB1 mediate activation of hepatic AMP-protein kinase (AMPK) and sirtuin1 (SIRT1) after Roux-en-Y gastric bypass in obese rats? J Gastrointest Surg 14: 221–228.

Peschechera A, Eckel J (2013). "Browning" of adipose tissue–regulation and therapeutic perspectives. Arch Physiol Biochem 119: 151–160.

Pulinilkunnil T, He H, Kong D, Asakura K, Peroni OD, Lee A *et al.* (2011). Adrenergic regulation of AMP-activated protein kinase in brown adipose tissue in vivo. J Biol Chem 286: 8798–8809.

Qiang L, Wang L, Kon N, Zhao W, Lee S, Zhang Y*et al.* (2012). Brown remodeling of white adipose tissue by SirT1-dependent deacetylation of Ppargamma. Cell 150: 620–632.

Raney MA, Turcotte LP (1985). (2008). Evidence for the involvement of CaMKII and AMPK in Ca2 + -dependent signaling pathways regulating FA uptake and oxidation in contracting rodent muscle. J Appl Physiol 104: 1366–1373.

Ren J (2004). Leptin and hyperleptinemia – from friend to foe for cardiovascular function. J Endocrinol 181: 1–10.

Rosell M, Kaforou M, Frontini A, Okolo A, Chan YW, Nikolopoulou E *et al.* (2014). Brown and white adipose tissues: intrinsic differences in gene expression and response to cold exposure in mice. Am J Physiol Endocrinol Metab 306: E945–E964.

Saito M (2015). Capsaicin and related food ingredients reducing body fat through the activation of TRP and brown fat thermogenesis. Adv Food Nutr Res 76: 1–28.

Schweiger M, Eichmann TO, Taschler U, Zimmermann R, Zechner R, Lass A (2014). Measurement of lipolysis. Methods Enzymol 538: 171–193.

Seale P, Bjork B, Yang W, Kajimura S, Chin S, Kuang S *et al.* (2008). PRDM16 controls a brown fat/skeletal muscle switch. Nature 454: 961–967.

Servera M, Lopez N, Serra F, Palou A (2014). Expression of "brown-in-white" adipocyte biomarkers shows gender differences and the influence of early dietary exposure. Genes Nutr 9: 372.

Shabalina IG, Petrovic N, de Jong JM, Kalinovich AV, Cannon B, Nedergaard J (2013). UCP1 in brite/beige adipose tissue mitochondria is functionally thermogenic. Cell Rep 5: 1196–1203.

Shan T, Liu W, Kuang S (2013). Fatty acid binding protein 4 expression marks a population of adipocyte progenitors in white and brown adipose tissues. FASEB J 27: 277–287.

Shen QW, Zhu MJ, Tong J, Ren J, Du M (2007). Ca^{2+}/calmodulin-dependent protein kinase kinase is involved in AMP-activated protein kinase activation by alpha-lipoic acid in C2C12 myotubes. Am J Physiol Cell Physiol 293: C1395–C1403.

Southan C, Sharman JL, Benson HE, Faccenda E, Pawson AJ, Alexander SPH *et al.* (2016). The IUPHAR/BPS Guide to PHARMACOLOGY in 2016: towards curated quantitative interactions between 1300 protein targets and 6000 ligands. Nucl Acids Res 44 (Database Issue): D1054–D1068.

Tian L, Wang C, Hagen FK, Gormley M, Addya S, Soccio R *et al.* (2014). Acetylation-defective mutant of PPARgamma is associated with decreased lipid synthesis in breast cancer cells. Oncotarget 5: 7303–7315.

Tramontana M, Giuliani S, Valenti C, Cialdai C, Lazzeri M, Turini D *et al.* (2009). Excitatory and inhibitory urinary bladder reflexes induced by stimulation of cervicovaginal capsaicin-sensitive sensory fibers in rats. Naunyn Schmiedebergs Arch Pharmacol 379: 107–114.

Turdi S, Kandadi MR, Zhao J, Huff AF, Du M, Ren J (2011). Deficiency in AMP-activated protein kinase exaggerates high fat diet-induced cardiac hypertrophy and contractile dysfunction. J Mol Cell Cardiol 50: 712–722.

van Beekum O, Fleskens V, Kalkhoven E (2009). Posttranslational modifications of PPAR-gamma: fine-tuning the metabolic master regulator. Obesity (Silver Spring) 17: 213–219.

Van De Kamer JH, Ten Bokkel Huinink H, Weyers HA (1949). Rapid method for the determination of fat in feces. J Biol Chem 177: 347–355.

Villanueva CJ, Vergnes L, Wang J, Drew BG, Hong C, Tu Y*et al.* (2013). Adipose subtype-selective recruitment of TLE3 or PRDM16 by PPARgamma specifies lipid storage versus thermogenic gene programs. Cell Metab 17: 423–435.

Vosselman MJ, van Marken Lichtenbelt WD, Schrauwen P (2013). Energy dissipation in brown adipose tissue: from mice to men. Mol Cell Endocrinol 379: 43–50.

Whittle AJ, Carobbio S, Martins L, Slawik M, Hondares E, Vazquez MJ *et al.* (2012). BMP8b increases brown adipose tissue thermogenesis through both central and peripheral actions. Cell 149: 871–885.

Wu J, Bostrom P, Sparks LM, Ye L, Choi JH, Giang AH *et al.* (2012). Beige adipocytes are a distinct type of thermogenic fat cell in mouse and human. Cell 150: 366–376.

Wu J, Cohen P, Spiegelman BM (2013). Adaptive thermogenesis in adipocytes: is beige the new brown? Genes Dev 27: 234–250.

Yagi S, Kadota M, Aihara K, Nishikawa K, Hara T, Ise T*et al.* (2014). Association of lower limb muscle mass and energy expenditure with visceral fat mass in healthy men. Diabetol Metab Syndr 6: 27.

Yehuda-Shnaidman E, Buehrer B, Pi J, Kumar N, Collins S (2010). Acute stimulation of white adipocyte respiration by PKA-induced lipolysis. Diabetes 59: 2474–2483.

Yoneshiro T, Saito M (2013). Transient receptor potential activated brown fat thermogenesis as a target of food ingredients for obesity management. Curr Opin Clin Nutr Metab Care 16: 625–631.

Yoshioka M, St-Pierre S, Drapeau V, Dionne I, Doucet E, Suzuki M *et al.* (1999). Effects of red pepper on appetite and energy intake. Br J Nutr 82: 115–123.

Yu Q, Wang Y, Yu Y, Li Y, Zhao S, Chen Y*et al.* (2012). Expression of TRPV1 in rabbits and consuming hot pepper affects its body weight. Mol Biol Rep 39: 7583–7589.

Zhang LL, Yan Liu D, Ma LQ, Luo ZD, Cao TB, Zhong J *et al.* (2007). Activation of transient receptor potential vanilloid type-1 channel prevents adipogenesis and obesity. Circ Res 100: 1063–1070.

Zhang X, Daugherty SL, de Groat WC (2011). Activation of CaMKII and ERK1/2 contributes to the time-dependent potentiation of Ca^{2+} response elicited by repeated application of capsaicin in rat DRG neurons. Am J Physiol Regul Integr Comp Physiol 300: R644–R654.

Zhou X, Zheng F, Moon C, Schluter OM, Wang H (2012). Bi-directional regulation of CaMKIIalpha phosphorylation at Thr286 by NMDA receptors in cultured cortical neurons. J Neurochem 122: 295–307.

Supporting Information

Additional Supporting Information may be found in the online version of this article at the publisher's web-site:

http://dx.doi.org/10.1111/bph.13514

Figure S1 [A]. Micrographs represent low magnification of Oil Red O staining of subcutaneous adipocytes isolated from NCD or HFD (CAP)-fed wild type (top) and TRPV1$^{-/-}$ (Bottom) mice (n = 40). [B]. Glycerol secreted per mg of protein per hour. measured in inguinal adipocytes of NCD or HFD (± CAP)-fed wild type and TRPV1$^{-/-}$ mice (n = 40). [C]. Basal and forskolin-stimulated glycerol release from WAT of WT and TRPV1$^{-/-}$ mice (n = 6). [D]. Coomassie blue staining for gel showing equal loading of proteins from EF lysate. [E]. Western blot showing the expression of FABP-4 in the isolated preadipocytes. [F]. The quantification of the FABP4/GAPDH ratio (means ± SEM). ** $P < 0.05$.